PROCEEDINGS OF SPIE

SPIEDigitalLibrary.org/conference-proceedings-of-spie

VIRUS: first deployment of the massively replicated fiber integral field spectrograph for the upgraded Hobby-Eberly Telescope

Hill, Gary, Tuttle, Sarah, Vattiat, Brian, Lee, Hanshin, Drory, Niv, et al.

Gary J. Hill, Sarah E. Tuttle, Brian L. Vattiat, Hanshin Lee, Niv Drory, Andreas Kelz, Jason Ramsey, Trent W. Peterson, D. L. DePoy, J. L. Marshall, Karl Gebhardt, Taylor Chonis, Gavin Dalton, Daniel Farrow, John M. Good, Dionne M. Haynes, Briana L. Indahl, Thomas Jahn, Hermanus Kriel, Francesco Montesano, Harald Nicklas, Eva Noyola, Travis Prochaska, Richard D. Allen, Ralf Bender, Guillermo Blanc, Maximilian H. Fabricius, Steve Finkelstein, Martin Landriau, Phillip J. MacQueen, M. M. Roth, R. D. Savage, Jan M. Snigula, Heiko Anwad, "VIRUS: first deployment of the massively replicated fiber integral field spectrograph for the upgraded Hobby-Eberly Telescope," Proc. SPIE 9908, Ground-based and Airborne Instrumentation for Astronomy VI, 99081H (9 August 2016); doi: 10.1117/12.2231064

SPIE.

Event: SPIE Astronomical Telescopes + Instrumentation, 2016, Edinburgh, United Kingdom

VIRUS: first deployment of the massively replicated fiber integral field spectrograph for the upgraded Hobby-Eberly Telescope*

Gary. J. Hill[a,b†], Sarah E. Tuttle[a], Brian L. Vattiat[a], Hanshin Lee[a], Niv Drory[a], Andreas Kelz[d,e], Jason Ramsey[a], Trent W. Peterson[a], D.L. DePoy[c], J.L. Marshall[c], Karl Gebhardt[b], Taylor Chonis[b], Gavin Dalton[j], Daniel Farrow[f], John M. Good[a], Dionne M. Haynes[d,e], Briana L. Indahl[b], Thomas Jahn[d,e], Hermanus Kriel[a], Francesco Montesano[f], Harald Nicklas[l], Eva Noyola[a], Travis Prochaska[c], Richard D. Allen[c], Ralf Bender[f,g], Guillermo Blanc[h], Maximilian H. Fabricius[f], Steve Finkelstein[b], Martin Landriau[a], Phillip J. MacQueen[a], M.M. Roth[d,e], R.D. Savage[a], & Jan M. Snigula[f], Heiko Anwad[l],

[a] McDonald Observatory, [b]Department of Astronomy, University of Texas at Austin, 2515 Speedway, C1402, Austin, TX 78712, USA

[c] Department of Physics and Astronomy, Texas A&M University, 4242 TAMU, College Station, TX 77843, USA

[d] Leibniz Institute for Astrophysics (AIP), An der Sternwarte 16, 14482 Potsdam, Germany

[e] innoFSPEC Potsdam, An der Sternwarte 16, 14482 Potsdam, Germany

[f] Max-Planck-Institut für Extraterrestriche-Physik, Giessenbachstrasse, D-85748 Garching b. München, Germany

[g] Universitäts-Sternwarte München, Scheinerstr. 1 , 81679 München, Germany

[h] Observatories of the Carnegie Institution for Science, 813 Santa Barbara Street, Pasadena, CA 91101, USA

[j] Department of Physics, Oxford University, Keble Road, Oxford, OX1 3RH, UK

[l] Institut für Astrophysik Göttingen, Friedrich-Hund-Platz 1, 37077 Göttingen, Germany

ABSTRACT

The Visible Integral-field Replicable Unit Spectrograph (VIRUS) consists of 156 identical spectrographs (arrayed as 78 pairs) fed by 35,000 fibers, each 1.5 arcsec diameter, at the focus of the upgraded 10 m Hobby-Eberly Telescope (HET). VIRUS has a fixed bandpass of 350-550 nm and resolving power R~700. VIRUS is the first example of industrial-scale replication applied to optical astronomy and is capable of surveying large areas of sky, spectrally. The VIRUS concept offers significant savings of engineering effort, cost, and schedule when compared to traditional instruments.

The main motivator for VIRUS is to map the evolution of dark energy for the Hobby-Eberly Telescope Dark Energy Experiment (HETDEX‡), using 0.8M Lyman-alpha emitting galaxies as tracers. The VIRUS array is undergoing staged deployment during 2016 and 2017. It will provide a powerful new facility instrument for the HET, well suited to the survey niche of the telescope, and will open up large spectroscopic surveys of the emission line universe for the first time. We will review the production, lessons learned in reaching volume production, characterization, and first deployment of this massive instrument.

Keywords: Telescopes: Hobby-Eberly, Astronomical instrumentation: Spectrographs, Spectrographs: VIRUS, Spectrographs: Integral Field, Spectrographs: performance

---

* The Hobby – Eberly Telescope is operated by McDonald Observatory on behalf of the University of Texas at Austin, Pennsylvania State University, Ludwig-Maximillians-Universität München, and Georg-August-Universität, Göttingen

† G.J.H.: E-mail: hill@astro.as.utexas.edu

‡ http://hetdex.org/

Ground-based and Airborne Instrumentation for Astronomy VI, edited by Christopher J. Evans, Luc Simard, Hideki Takami
Proc. of SPIE Vol. 9908, 99081H · © 2016 SPIE · CCC code: 0277-786X/16/$18 · doi: 10.1117/12.2231064

1. INTRODUCTION: HET WIDE FIELD UPGRADE AND VIRUS

Large, targeted, spectroscopic surveys of continuum-selected objects are now becoming the norm, and have greatly increased our understanding in many areas of astronomy. Surveys of the emission-line universe, however, are limited currently to wide field imaging with narrow band filters, or to narrower fields with Fabry-Perot etalons or adaptations of imaging spectrographs. Integral field (IF) spectrographs offer a huge gain over these techniques, depending on the application, providing greater sensitivity and wavelength coverage as well as true spectroscopy. The current generation of IF spectrographs is well-adapted to arcminute-scale fields of view, with several thousand spatial elements, and adequate spectral coverage for targeted observations of individual extended objects. They have the grasp to detect simultaneously of order 0.5 million (spectral x spatial) resolution elements.

1.1 Large-scale replication of VIRUS

In order to undertake large-scale surveys for emission-line objects, much greater field coverage is needed. Narrow-band imaging surveys can now cover large areas, but often require spectroscopic follow-up, and still do not probe sufficient volume to detect rare objects or to overcome cosmic variance. Wide-field IF spectroscopy requires a large multiplexing factor, so we have embarked on a program to produce an instrument that uses large-scale replication to create a unique astronomical facility capable of spectroscopic surveys of hundreds of square degrees of sky[1]. The instrument is the Visible Integral-field Replicable Unit Spectrograph (VIRUS)[1-6], a simple, modular integral field spectrograph that is being replicated 156-fold, to provide an order of magnitude increase in grasp (AΩ) over any existing spectrograph, when mounted on the upgraded Hobby-Eberly Telescope (HET)[7-11]. Fig. 1 shows the upgraded HET as it now appears.

The traditional astronomical instrument has a monolithic design and is a one-off prototype, where a large fraction of the cost is expended on engineering effort. When compared to monolithic instruments, there are cost savings from creating several copies of a spectrograph to gain multiplex advantage, because the components are less expensive and the engineering is amortized over the production run. As an example, the new MUSE[12] instrument for ESO VLT field-slices a 1 arcmin. square field into 24 duplicated IF spectrographs. VIRUS makes the next step, and exploits industrial-scale replication, which we (arbitrarily) define to be in excess of 100 spectrograph channels. We build upon the concepts laid out in Refs. 1-4, where we concluded that industrial-scale replication offers significant cost-advantages when compared to a traditional monolithic spectrograph, particularly in the cost of the optics and engineering effort. This concept breaks new ground in optical instruments, and appears to be a cost-effective approach to outfitting the coming generation of ELTs, for certain instrument types, where the multiplex advantage of an integral field can avoid growth in the scale of instruments with telescope aperture[1].

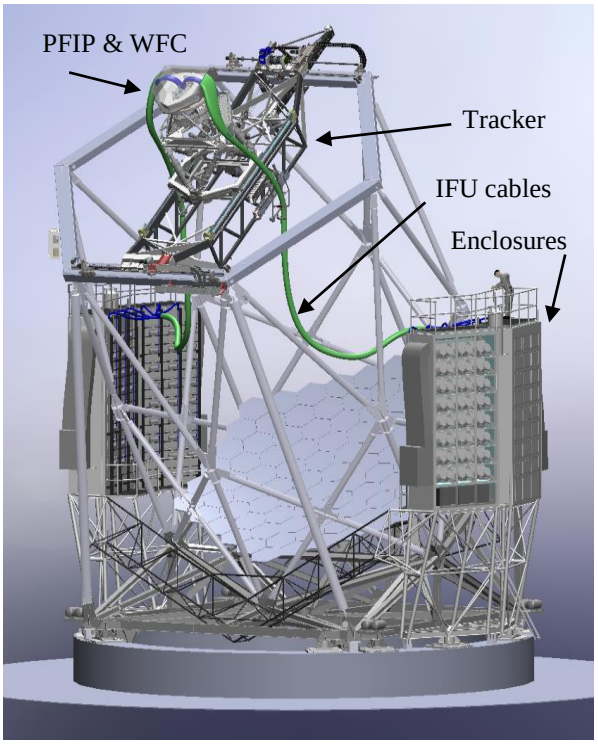

Figure 1 – Upgraded HET. The new tracker supports the Wide Field Corrector (WFC) and Prime Focus Instrument Package (PFIP). The IFU fiber cables run about 20 m to the two enclosures on the VIRUS Support Structure with Cryogenic System that house the 78 pairs of integral field spectrographs that make up VIRUS and the two units of LRS2.

The motivation for VIRUS is the Hobby-Eberly Telescope Dark Energy Experiment (HETDEX[6,13]), which will map the spatial distribution of about 0.8 million Lyα emitting galaxies (LAEs) with redshifts $1.9 < z < 3.5$ over a 420 sq. deg. area (9 Gpc^3) in the north Galactic cap and an equatorial field, using VIRUS on the upgraded HET. This dataset will constrain the expansion history of the Universe to 1% and provide significant constraints on the evolution of dark energy. The advantage of an IF spectrograph for this project is that the tracer galaxies are identified and have their redshifts determined in one observation.

The design of VIRUS flows directly from the requirements for HETDEX, to maximize the number of LAEs detected in a

set observing time, and to span sufficient redshift range to survey the required volume. These science requirements flow down to the following technical requirements for VIRUS:

- Coverage of $\Delta z \sim 2$ and coverage into the ultraviolet to detect LAEs at the lowest possible redshift. VIRUS is designed for $350 < \lambda < 550$ nm or $1.9 < z < 3.5$
- Resolution matching the linewidth of LAEs (R~700) to maximize detectability.
- Minimum throughput on sky (including atmosphere) ranging between 5% at 350 nm, 15% at 450 nm, and 10% at 550 nm to reach sensitivity of $3\text{-}4 \times 10^{-17}$ erg/cm^2/s in 20 minutes on HET.
- Low read noise detector (~3 electrons) to achieve sky-background dominated observations in 360 seconds
- High stability to ambient temperature variations, though not to gravity variations since the VIRUS modules will be fixed on HET.
- Simple, inexpensive design.

Each VIRUS unit is fed by 448 fibers that each cover 1.8 arcsec^2 on the sky, arrayed in two spectrograph channels. The fibers feeding a two-channel unit are arrayed in a 50×50 arcsec^2 IFU with a 1/3 fill-factor. A dither pattern of three exposures fills in the area. The spectral resolution is 0.60 nm (R~750 at 450 nm), with coverage of 350–550 nm. The optical design is simple, using three reflective and two refractive elements. With dielectric reflective coatings optimized for the wavelength range, high throughput is obtained. The full VIRUS array will simultaneously observe 35,000 spectra with 14 million resolution elements. In total, VIRUS has 0.7 Gpixels, comparable to the largest imagers yet deployed. The IFUs are arrayed within the 22′ field of the upgraded HET with ~1/4.5 fill factor, sufficient to detect the required density of LAEs for HETDEX. Development started with the prototype Mitchell Spectrograph (formerly VIRUS-P[3]), deployed in October 2006, and the production prototype where value engineering were used to reduce the cost for production. VIRUS is now approaching the end of production, and we present here results from the first deployment of 16 units on the upgraded HET. VIRUS is a joint project of the University of Texas at Austin (UT Austin), Leibniz-Institut für Astrophysik Potsdam (AIP), Texas A&M University (TAMU), Max-Planck-Institut für Extraterrestriche-Physik (MPE), Ludwig-Maximilians-Universität München, Pennsylvania State University, Institut für Astrophysik Göttingen, University of Oxford, Max-Planck-Institut für Astrophysik (MPA), and The University of Tokyo.

1.2 The Hobby-Eberly Telescope and Wide Field Upgrade

The HET is an innovative telescope with an 11 m hexagonal-shaped spherical mirror made of 91 1-m hexagonal segments that sits at a fixed zenith angle of 35º. HET can be moved in azimuth to access about 70% of the sky visible at McDonald Observatory ($\delta = -10.3^o$ to $+71.6^o$). The pupil sweeps over the primary mirror as the x-y tracker follows objects for between 50 minutes (in the south at $\delta = -10.0^o$) and 2.8 hours (in the north at $\delta = +67.2^o$). The maximum time on target per night is 5 hours and occurs at $+63^o$.

The HET was originally envisioned as a spectroscopic survey telescope, able to efficiently survey objects over wide areas of sky. While the telescope was very successful at observing large samples of objects such as QSOs spread over the sky with surface densities of around one per 10 sq. degrees, the HET design coupled with the very limited field of view of the corrector hampered programs where objects have higher sky densities. In seeking a strong niche for the HET going forward, we initiated a wide field upgrade to increase the field of view to 22 arcmin, coupled with a highly multiplexed spectrograph in order to exploit the strengths of the telescope and of the site.

The requirement to survey large areas of sky with VIRUS plus the need to acquire wavefront sensing stars to provide full feedback on the tracker position led us to design a new corrector employing meter-scale aspheric mirrors and covering a 22-arcmin diameter field of view. The HET Wide Field Upgrade (WFU[7-11]) is now in operation with the wide field corrector (WFC[14-16]), the new tracker[9,17], prime focus instrument package (PFIP[18,19]), and software and metrology systems[20-23]. The WFC has improved image quality and a 10 m pupil diameter. The periphery of the field is used for guiding and wavefront sensing to provide the necessary feedback to keep the telescope aligned as it tracks. The WFC has 30 times larger observing area than the old HET corrector. The WFC was manufactured by the University of Arizona College of Optical Sciences (OSC), and was delivered in May 2015[16].

The new tracker was needed to accommodate the size and five-fold weight increase of the new PFIP and WFC. It represents a third generation evolution of the trackers for HET and SALT, and is in essence a precision six-axis stage. The tracker was developed by McDonald Observatory (MDO) and the Center for Electro-Mechanics (CEM) at the University of Texas at Austin[9,17]. Deployment started in late 2013, following removal of the previous tracker.

HET requires constant monitoring and updating of the position of its components in order to deliver good images. The WFC must be positioned to 10 μm precision in focus and X,Y, and 4.0 arcsec in tip/tilt with respect to the optical axis of the primary mirror. This axis changes constantly as the telescope tracks, following the sidereal motions of the stars. Tilts of the WFC cause comatic images. In addition, the global radius of curvature of the primary mirror can change with temperature (as it is essentially a glass veneer on a steel truss), and needs to be monitored. The segment alignment maintenance system (SAMS) maintains the positions of the 91 mirrors with respect to each other, but is less sensitive to the global radius of curvature of the surface. The feedback to maintain these alignments requires excellent metrology, which is provided by the following subsystems:

- Two guide probes to monitor the position on the sky, and plate scale of the optical system, and monitor the image quality and atmospheric transparency
- Two Shack-Hartmann (S-H) wavefront sensors (WFS) to monitor the focus and tilt of the WFC, and seeing
- Distance measuring interferometer (DMI) to maintain the physical distance between the WFC and primary mirror
- Tip-tilt sensor (TTS) to monitor the tip/tilt of the WFC with respect to the optical axis of the primary mirror

The upgrade adds wavefront sensing[7,8,21-23] to HET in order to close the control loop on all axes of the system, in conjunction with the DMI and TTS adapted from the current tracker metrology system. There is redundancy built into the new metrology system in order to obtain the highest reliability. Two guide probes distributed around the periphery of the field of view provide feedback on position, rotation, and plate scale, as well as providing a record of image quality and transparency. The alignment of the corrector is monitored by the wavefront sensors as well as by the DMI and TTS. The radius of curvature of the primary mirror is monitored by the combination of focus position from the WFS with the physical measurement from the DMI and checked by the plate scale measured from the positions of guide stars on the guide probes. The SAMS edge-sensors provide a less sensitive but redundant feedback on radius of curvature as well. The PFIP includes a calibration WFS, which provides the reference for telescope focus and a pupil viewing camera to monitor the primary mirror and throughput.

At the time of writing, the WFU is installed and performing very well, significantly better than the old HET[11]. Pointing and tracking are meeting specifications and 5-7 minute setup times are significantly faster than with the old system. The WFC produces excellent image quality over the full field[16].

The previous HET Low-Resolution Spectrograph[24] was incompatible with the WFU and will be replaced with a more capable broad-band fiber-fed instrument based on VIRUS, called LRS2[25,26]. It takes advantage of the fact that VIRUS was designed to be easily adapted to a wide range of spectral resolutions, and wavelength ranges by changing dispersers and optics coatings. LRS2 is fed by a 7x10 arcsec^2 lenslet coupled fiber IFU[27], covers 350-1100 nm, simultaneously at a fixed resolving power R~1800, with the wavelength range split with dichroics into four channels shared between two VIRUS units, one for the blue and red wavelength range (370 - 630 nm) and the other for the red and far-red range (630-1050 nm). It uses the multiplex power of VIRUS to cover wavelength, rather than wide area. Only minimal modification from the base VIRUS design in gratings (grisms for both units) and in the detectors (to thicker CCDs for the far-red unit only) was required. LRS2 is the first facility instrument to be deployed on the upgraded HET, and it is now in science operations. LRS2 is a powerful instrument serving the HET strengths in survey follow-up, synoptic observations, and transient events. It will be particularly useful for following up emission-line objects detected with VIRUS at higher resolution, and can be used in parallel with VIRUS.

3. VIRUS PRODUCTION DESIGN

Before embarking on the replication of VIRUS units we built a prototype. The motivation for building the VIRUS prototype (Mitchell Spectrograph, formerly VIRUS-P[3]) was to provide an end-to-end test of the concepts behind HETDEX, both instrumental and scientific. Construction and testing of the prototype have verified the opto-mechanical design, the throughput, the sensitivity, and demonstrated the utility of such an instrument for surveys of emission-line objects. It has also served as a test-bed for the software development needed for analyzing the data from the full VIRUS array. The parallel nature of VIRUS means that the prototype can be used to develop the final software pipeline. The Mitchell Spectrograph was also designed to be a facility instrument on the McDonald 2.7 m Smith Telescope (HJST). On the HJST at f/3.65, the 200 μm fiber cores subtend 4.1 arcsec, and the IFU covers 3.5 arcmin^2. While the fibers are large, projected on the sky, the IFU covers the largest area of any current IF spectrograph and this results in great sensitivity for wide area surveys and particularly for spatially extended low surface brightness emission[28]. The Mitchell Spectrograph was used for a pilot survey of Ly-α emitting galaxies in support of the HETDEX project (HPS[29,30]). The results of the HPS confirm the

sensitivity estimates on which HETDEX is based[29], and demonstrate the effectiveness of blind IFU spectroscopy for this application.

The VIRUS instrument consists of three basic sub-units: the IFU, the collimator/grating assembly, and the camera assembly. The beam size is 125 mm, allowing the collimator to accept an f/3.32 beam from the fibers, accommodating a small amount of focal ratio degradation of the f/3.65 input from the telescope. The camera is a f/1.33 vacuum Schmidt design with a 2k x 2k format CCD with 15 μm pixels at its internal focus. Evolution of the design of VIRUS from the prototype to the production model was made in two steps. First a pre-production prototype was developed that incorporated the production engineering to reduce costs. In particular aluminum and Invar castings for components including the cryostat were prototyped and qualified. Second, small design modifications gleaned from this experience were incorporated into the First Article production unit and that was followed by production of an initial batch of 2 units which became references for production of IFUs, collimators and cameras in different locations[4].

The IFU, collimator, and camera subsystems have kinematic interfaces between them. Cameras are being produced at UT Austin[31], collimators at TAMU[32], and IFUs at AIP[33-35]. Oxford University provided a large number of mechanical parts for the collimators and cameras, and IAG has manufactured many IFU components and the input head mount plate that mounts them to the telescope. Spectrograph integration, alignment, and characterization is led by UT Austin[36].

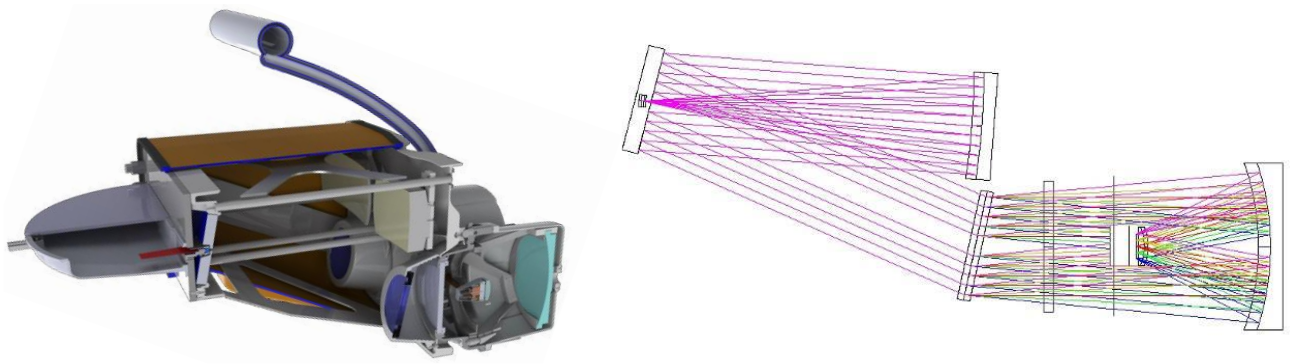

Figure 2: Layout of the production VIRUS. Left shows the production mechanical design and right shows the optical design. The grating has 930 l/mm and the coverage is fixed at 350-550 nm. The mechanical cutaway shows the IFU slit assembly on the left, mounted to the collimator. The Schmidt camera has an internal CCD in the vacuum and mounts to the main bulkhead of the collimator. It is cooled by a flexible line from above with a breakable cryogenic bayonet connection.

3.1 VIRUS Production Optomechanical Design

While the VIRUS units are mounted in fixed housings, their enclosures track ambient temperature and they are required to operate with high stability under a wide range of temperature from -5 to +25 degrees Celsius. The instrument is specified to not require recalibrating for shifts in the positions of the fiber spectra over the temperature range encountered in an hour, with the goal of maintaining alignment during an entire night. Stability is crucial since the data reduction and analysis is sensitive to 0.1 pixel shifts in the spectra. This requirement corresponds to shifts smaller than 0.5 pixels (1/10 of a resolution element) at the detector for 5 degrees Celsius temperature change. The Mitchell Spectrograph was designed to test this requirement. It is mounted in a gimbal to maintain its orientation, but sees the full temperature swing in a night.

For production, we made some significant changes to the design, based on experience with the Mitchell Spectrograph and responding to the development for the HET WFU design. The most significant was to double the spectrographs so that a pair shares a single IFU, a common collimator housing, and a common cryostat (Fig. 2). The motivation for this came first from fiber cable handling: it is more efficient in terms of weight and cross-sectional area to double the number of fibers in a cable (note that the fiber itself is not the dominant weight in a bundle). There is not a significant cost-savings on the IFU, since the majority of the cost is in the fiber, but volume occupied by the cables is reduced and the cable handling becomes significantly easier with 78 instead of 156 cables to accommodate. The other advantage to the double unit is that two cameras share a vacuum, and have a single connection to the liquid nitrogen (LN) cooling system. This increases the evacuated volume in an individual cryostat, which increases hold-time, and saves cost on vacuum valves and other fixturing. Pairing the spectrographs enabled reduction of mechanical structure to support optics by eliminating the redundant structure of two spectrographs placed side-by-side. The complexity of the enclosures to house the spectrographs

was also reduced by pairing the instruments because fewer interfacial features between instrument and superstructure are required.

The optical layout was modified to make the system more linear and allow the units to be packed more tightly in the housings (Fig. 2). Analysis of the fiber diameter for maximizing the number of Lyman-α emitting (LAE) galaxies detected by the HETDEX survey indicates that the ideal is 1.5 arcsec for the expected range of image quality to be encountered in the survey (1.3 to 1.8 arcsec FWHM). Analysis of the expected number of LAEs with redshift also indicates that the majority of the objects are located at $z<3.5$ due to the change in distance modulus with redshift coupled with the steepness of the LAE luminosity function. As a result, the decision has been made to reduce the wavelength coverage so as to preserve spectral resolution, while accommodating the larger fibers (266 vs 200 μm core diameter). This is a small change and the increase in dispersion of the grating (930 versus 830 l/mm used for the HPS) does not effect diffraction efficiency over the observed bandpass. Wavelength coverage is 350 – 550 nm ($1.9 < z < 3.5$) and resolving power is R=700 at 450 nm.

Figure 3 shows an exploded view of the spectrograph unit. The VIRUS optics and mechanical interfaces were carefully specified to produce optics that will be interchangeable amongst any VIRUS unit. Both the optical and mechanical properties of each optic have been carefully toleranced using Monte Carlo realizations of the collimator and camera that were then combined and evaluated. The optical tolerancing is described in detail in Ref 37. Particular attention was paid to the relative alignment of the axes of the two spectrographs within a single unit.

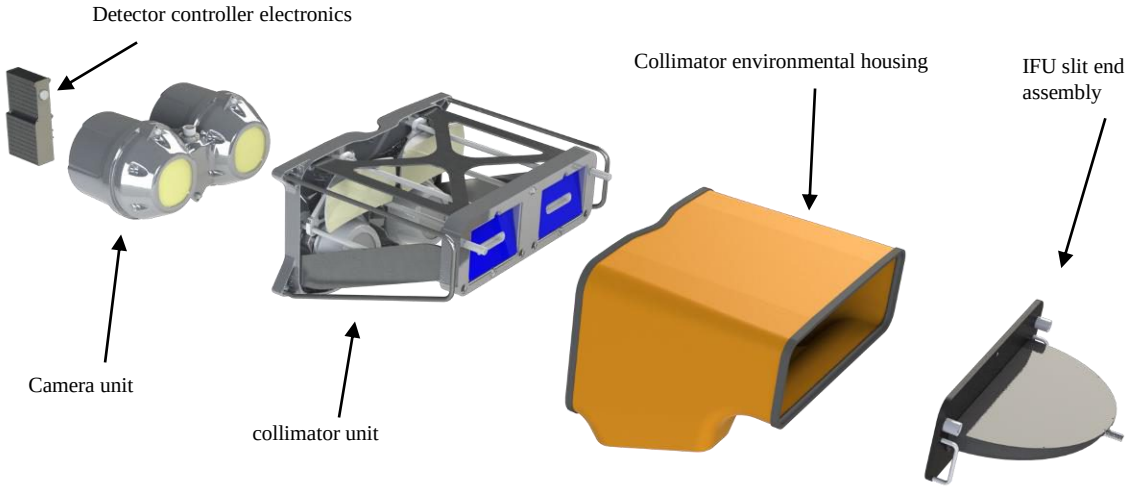

Figure 3. Basic components of the VIRUS unit housing two spectrographs. Light enters at the IFU slit assembly along two axes. The collimator holds the IFU and camera cryostat on kinematic mounts and forms the main structure of the instrument. The cameras are interchangeable and removable should maintenance be required. The detector controllers mount directly to the cryostats.

Detailed information on the VIRUS mechanical design is given in Refs 38-40. Kinematic mounts enable highly repeatable registration between components and their use is prevalent in precision optical assemblies. The VIRUS spectrograph relies on kinematic mounts between sub-assemblies, which are considered modular to each other, specifically the IFU slit assembly, the collimator, and the camera. The optical and mechanical tolerances of the instrument are arranged such that modules of a particular type would be interchangeable. For example, the camera couples to the collimator through a kinematic mount. Originally it was required that any camera could be used with any collimator and perform within specification. However, experience in alignment led us to instead allow both camera and collimator mirrors to be adjusted, leading to better than specification image quality at the expense of making the camera and collimator matched for a given spectrograph unit. Similarly, the VPH gratings are modular to the collimator and the detector sub-assemblies are modular to the camera body. Collimators and gratings were assembled at TAMU, mainly using student labor from parts supplied by Oxford, UT, and TAMU[32]. The fold flats were integrated into the front bulkhead with a simple centering grid and glued in place with epoxy. Assembly of the mechanical structure took on the order of an hour. A Faro CMM arm is used for alignment of the optics to within 100 μm tolerance. The gratings are glued into their cells and set for rotation in their housings. 61 production collimator units were assembled at TAMU and the remainder are being assembled at UT Austin.

3.2 VPH Gratings

VIRUS uses volume phase holographic (VPH) gratings, which offer high efficiency and low cost. The setup for HETDEX employs VPH gratings with physical dimensions of 148 mm in diameter by 16 mm in total thickness; the VPH layer itself has a 138 mm diameter clear aperture and is sandwiched between two 8 mm thick, anti-reflection (AR) coated fused silica substrates using an optical grade adhesive. The grating has a fringe frequency of 930 lines/mm and operates at order m = 1 in transmission from 350 to 550 nm for unpolarized light. Efficiency is optimized for the UV by lowering the angle of incidence away from the Bragg angle, which is close to 12 degrees.

Details of the grating design, development, and testing are reported in Refs. 41 & 42. We undertook tests of small and full size gratings from Wasatch Photonics, Kaiser Optical Systems International (KOSI), and SyZyGy using a custom automated test-bench that can fully characterize a grating over a range of input and output angles. This test bench was used to evaluate test gratings as it allows orders m=-1,0,1,2 to be measured to account for as much of the diffracted light as possible[41]. Performance in the ultraviolet was enhanced by reducing the angle of incidence to shift the blaze to the UV. Angle changes of the grating at fixed collimator angle have little effect on the wavelength range, so tilting the grating provides an independent free parameter in tuning the throughput as a function of wavelength. In addition, we specified a 1 deg. tilt of the fringes in the grating, to ensure that the "Litterow" recombination ghost[43] is off the detector for the VIRUS configuration.

In order to ensure a standardized reference for measurements of diffraction efficiency of production gratings compared to specifications, and to facilitate more rapid testing than possible with the flexible test bench mentioned above, we developed a simple rugged grating tester for the specific gratings we are procuring for VIRUS[42]. LEDs with wavelengths of 350,450, and 550 nm illuminate a 12.5 mm subaperture on the grating surface. A silicon photodiode fed by a beamsplitter normalized the light output of the LEDs. The angles of incidence and diffraction are fixed to the VIRUS configuration and the light is imaged onto a 2/3 format commercial CCD camera by an off-the-shelf aspheric lens. Calibration was provided by a fiducial grating that underwent a detailed characterization on our main grating test bench. Custom software and control allowed a grating to be tested in 10 minutes, including efficiency and scattered light. The position of the grating was moved laterally to sample 9 subapertures in order to provide an average efficiency more representative than spot measurements. We have found that VPH gratings exhibit quite significant small-scale variations in efficiency and it is possible to find and report a "hot-spot" in the diffraction efficiency, if too small an area is measured. This is particularly the case with laser measurements employed by some vendors. The grating tester was tailored to the properties we care about in the specification and avoided conflicts over inconsistent measurement methods between vendor and our lab. The contract for 170 gratings was awarded to SyZyGy and production results as gathered by the grating tester are reported in Ref. 42.

3.3 Camera Design and Detector System

The camera cryostat vacuum is shared between a pair of spectrographs. This modification effectively halves the number of ancillary vacuum components such as valves and vacuum gauges. This saves not only the expense of these components but reduces the number of sealing surfaces that contribute to long-term vacuum degradation and are a point of failure. The larger evacuated volume also leads to longer vacuum hold-time. Similarly, the cryogenic cooling system is shared within a unit. This reduces the part-count of the instrument cryogenic system and also simplifies the cryogenic distribution system and losses associated with fittings and valves. The cryogenic system development and testing is described in greater detail in Sec. 5 and Refs. 44,45. The cryostat is composed of two aluminum castings, post-machined only on critical mount surfaces and flanges. Cryostats were manufactured by MKS Inc., following extensive evaluation of prototypes. An impregnating step with Locktite Resinol, following machining, ensures that the porosity of the cast aluminum does not lead to virtual leaks or poor vacuum seals, and leak rates are achieved that are consistent with the O-ring length and internal volume of the cryostat. While the tooling cost for casting is quite significant, the cost for even a single cryostat of this size is competitive with machining from bulk stock, and is much cheaper for the VIRUS production run.

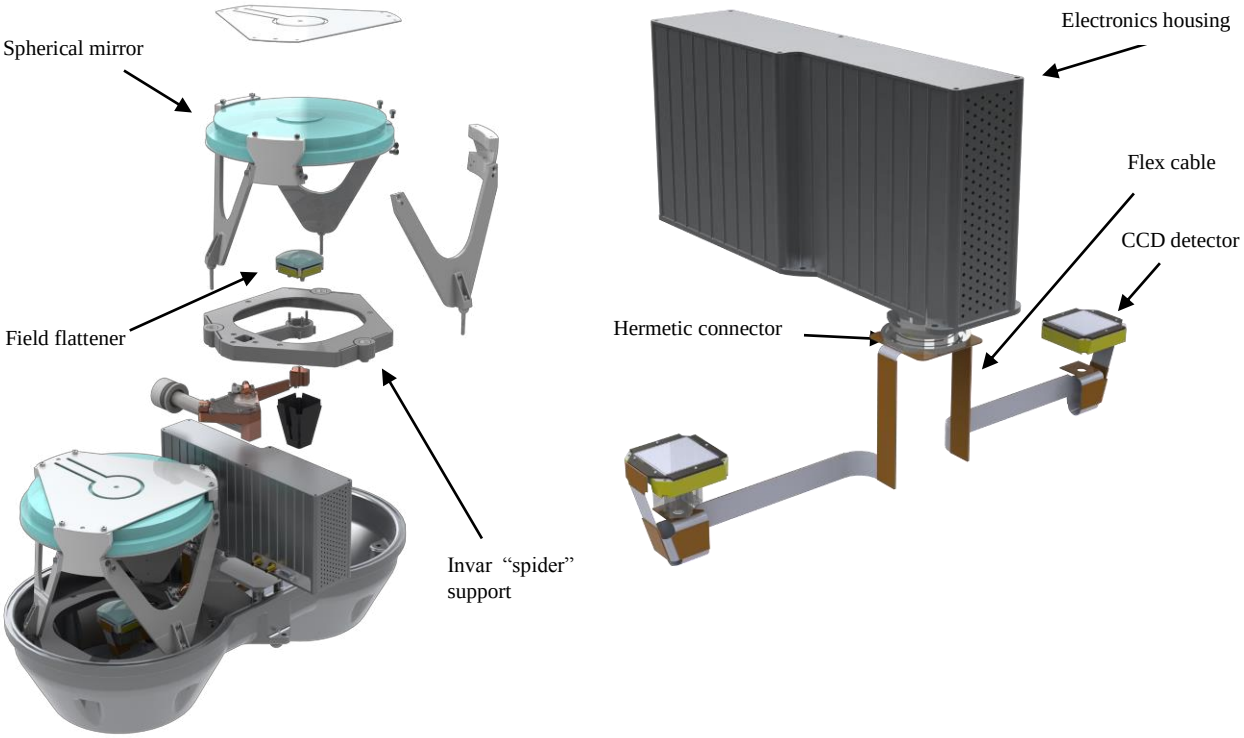

Figure 4. Camera assembly and electronics. Left shows the integration of the two camera channels into the cryostat. Right shows the detector system controller, the flex circuit, and the CCD packages as they integrate into the cryostat.

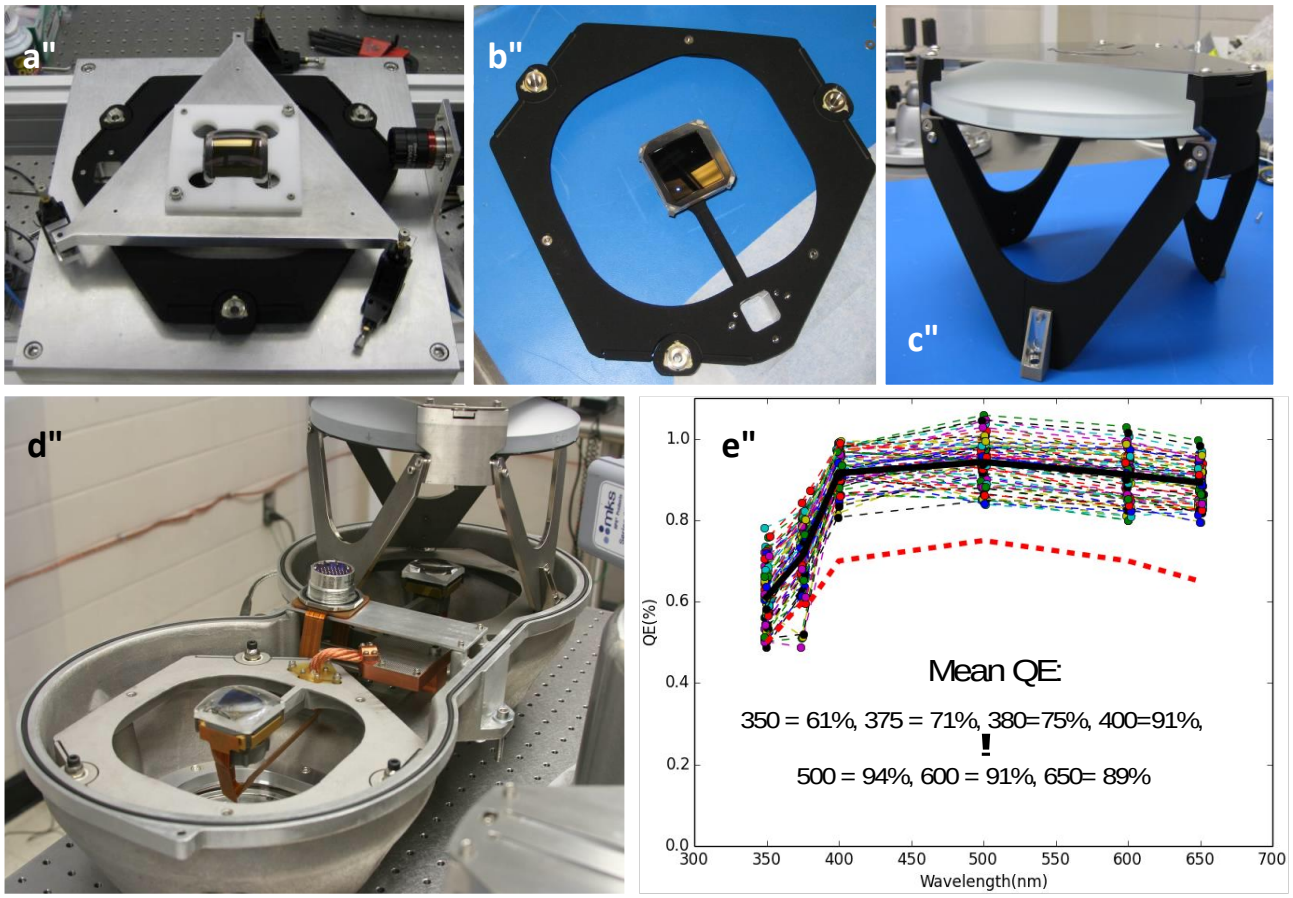

Figure 5. VIRUS camera production and detector performance. (a) alignment of field flattener lens to CCD detetector in custom jig; (b) assembled "spider" with detector and field flattener; (c) completed cameral mirror assembly ready for integration; (d) integration of cryostat (not fully metal finished first article); (e) statistics on quantum efficiency (QE) of delivered detectors – red dashed line is requirements, solid black line is mean of the batch.

at 20 seconds, binned 2x1, but low read noise (~3 electrons) is required and the parallel readout of 156 CCDs is still challenging. The VIRUS system is 665 Mpixel, which is comparable to MUSE[46] and to the largest imaging mosaics yet deployed. The data volume from the full VIRUS array is about 2.5 GB per observation. Observation times per field are 20 minutes for the HETDEX survey, split into three exposures, and we expect to generate 40 TB of raw data over the course of the survey, including calibrations.

The integrated detector system was supplied by Astronomical Research Cameras, Inc., with the University of Arizona Imaging Technology Laboratory providing thinned backside illuminated CCDs with AR coatings optimized for the VIRUS bandpass, as a subcontract from wafers manufactured by Semiconductor Technology Associates, Inc. Since the CCDs come from custom wafer runs, we elected to increase the imaging area to 2064 by 2064 pixels, allowing more latitude for alignment.

The design of the detector package, flex circuit, and controller were highly customized to the VIRUS application, since the engineering effort is spread over a large production run. This allowed us to remove most of the complexity associated with the detector head of the Mitchell Spectrograph. Figures 4 and 5 show the layout for a pair of detectors in a single cryostat. The CCD package, machined from Invar-36, is designed for minimum obstruction and hides in the shadow of the field flattener (FF) lens. The CCDs are flat to within +/-10 μm, which is allowed by the tolerance analysis. The package has a custom header board that brings the traces to a single connector on one side of the package. A custom flex circuit with complex geometry connects the two detectors to a single 55-pin hermetic bulkhead connector. The controller mounts directly to this connector, without cables, and its form-factor was customized to fit between the cylinders of the cryostat cover.

The CCD and FF alignment tolerances are the tightest in the system. Initially we aligned and bonded the FF in-situ[31], but this caused some deposition of epoxy in the corners of the CCDs during cure due to outgassing. We modified the procedure to provide separate alignment references for FF and CCD that allow the FF to be bonded to its mounts separately from the CCD. They are then brought together and the alignment between them confirmed by metrology with an alignment telescope. Once the FF lens is installed its optical axis defines the axis of the head and allows alignment of the mounts on the "spider" that interface with machined features within the camera cryostat. Since the camera mirror structure mounts to the same points, the entire camera becomes a unit with only the aspheric corrector plate (with much lower alignment tolerances) separate.

The detector package with attached FF is then integrated into the "spider" which supports the detector head, cantilevered in the beam. The spider is of post-machined cast Invar-36, and its production is discussed further in Ref. 31. The whole spider is adjusted in all degrees of freedom in an alignment jig to position the FF on the axis of a laser that defines the camera axis. Four lugs are then glued in place to capture the alignment, and they interface to machined features in the cryostat housing. In this way, the alignment of the CCD and FF to the axis of the camera is achieved within the required tolerances of 50 μm in centration and separation, and 0.05 degrees in tilt[37].

The shutter for the system is located in front of the IFU inputs, just below the focal surface in the PFIP[18,19]. It has a rotary blade design, and a minimum exposure time of 1 second. The shutter is located remotely from the detector controllers and is commanded separately. Exposures are coordinated via the Telescope Control System, which sends simultaneous shutter-open commands to the shutter control system and to the VIRUS Data Acquisition System (VDAS) that controls the detector system. Timing between the shutter and the VDAS is maintained with a Network Time Protocol server, synchronized to GPS time.

The CCD controllers have DC power in and fiber-optic data lines out. To minimize crosstalk, the timing of all CCD clocks is synchronized to a master clock signal distributed over a Low-Voltage Differential Signal (LVDS) system. The data system requires several levels of multiplexing. First, each CCD controller commands two detectors, each with two readout amplifiers. Next, a custom-built 8-way multiplexer combines the output from each set of 8 CCD controllers. Next, the output of each of 12 multplexers is fed into a PCI interface card. Two PCI-to-PCIe expansion chassis are used to connect 6 PCI interface cards each to a PCIe port in the VDAS computer. Finally, the data are transferred via DMA from the PCI interface cards into the VDAS memory.

3.4 Detector Status

When we commissioned the pixelflat head for characterization[36] (see below) that provides continuous illumination of a slit so that CCD pixel-to-pixel variations can be recorded, we noticed some instances of CCDs showing blemishes that were not present at delivery. These flaws fall into two categories: many small (few pixel diameter) regions of lower QE, particularly in the corners of the CCDs (which we call "pox"), and large-scale depression of the QE particularly in the center (which we call "depression"). Many CCDs appeared relatively unaffected, and some cryostats had one good CCD and one showing one or other of the degradations. The effect was highly variable, which made diagnosis difficult.

In consultation with ITL we traced the likely trigger of the depression degradation to residue of release agent on the storage boxes. About 20% of the CCDs show this failure, but all are likely contaminated. The cause of he pox was traced to components inside the VIRUS cryostats that had been stored in anti-tarnish bags after cleaning and not re-cleaned before integration. The response of a given CCD to these contaminants is highly variable, but many cameras have at least one CCD that is affected. ITL has demonstrated that the CCDs with pox can be cleaned by a cold plasma process, but the others seems not to respond as well. We are proceeding to clean or replace the CCDs and to clean and rebuild cameras in order to eliminate these problems, but this has set back deployment of VIRUS quite significantly.

Through characterization we have been able to identify 16 units that are affected only mildly and proceeded to deploy them at HET in order to advance the system integration, see below.

3.5 Integral field unit cables

For VIRUS we have elected to use a bare fiber bundle to maximize throughput and minimize cost[3,4,33-35]. The primary advantage of lenslets is in coupling the slower f/ratios of typical foci to the fast ratio required to minimize focal ratio degradation (FRD[47]), and such IFUs are ideal for retro-fitting existing spectrographs. Lenslets do not provide perfect images, however, so if there is flexibility to choose the input f/ratio to the fibers and if the fill-factor can be tolerated, trading it against total area, the bare bundle provides the best efficiency[2]. Also, the central obstruction of the telescope is preserved at the fiber output to large extent if there is low FRD. This is an advantage for a catadioptric camera as in VIRUS. For the VIRUS IFUs we use a fill factor of 1/3 for the fiber cores, with the fibers in a hexagonal close pack, and dither the IFU arrays through three positions to fill the area. Note that if the f/ratio of the microlens-coupled case is the same as the f/ratio from the telescope in the bare-fiber case, and the lenslets subtend the same area on the sky as the bare fibers at that f/ratio, then the fill-factor of the densepak type array is exactly offset by the larger area that the bundle covers per exposure. So in the case where maximum areal coverage is required, and especially with an obstructed catadioptric camera, the bare bundle is the preferred solution.

The HET site has a median seeing of 1.0 arcsec FWHM, and the upgraded HET is expected to deliver 1.3 arcsec images on average as required. Analysis of the trade-off between areal coverage and sensitivity shows that larger fibers are preferred for HETDEX to maximize both the volume surveyed and the number of detected LAE galaxies. As a result, 1.5 arcsec (266 μm) diameter fiber cores were adopted for the production VIRUS units. The WFC delivers f/3.65. The optics of VIRUS can accommodate an f/ratio of f/3.32 (within the 125 mm pupil size), allowing some focal ratio degradation and accommodation of alignment errors in the subsystems.

IFU development at the Leibniz Institute for Astrophysics (AIP)[33-35] and University of Texas at Austin (UT)[47,48] has focused on establishing a design that minimizes FRD, maximizes throughput, and is manufacturable in quantity[34]. Careful and rigorous apportioning of tolerances between the components aims to keep 95% of the transmitted light within the spectrograph pupil. Figure 6 shows images of the slit and input ends of production fiber cables. They each contain 448 fibers with 266 μm cores, and we have kept the design as simple and lightweight as possible. The input head consists of a precision micro-drilled block from Euro Micron into which the fibers are fed which is in turn clamped within a stainless steel shell that provides the mounting features. The fibers are glued in with epoxy and then cut off and polished. At the exit, the cable bifurcates within a slit housing into two slits with the fibers glued to grooved blocks of the same design as for the Mitchell Spectrograph. Input and output are bonded to a thin lens and a cylindrical lens, respectively, both of fused silica and AR coated. The lens on the input ensures the chief ray of the curved focal surface is normal to the fiber input for all the fibers, even though the input face is flat.

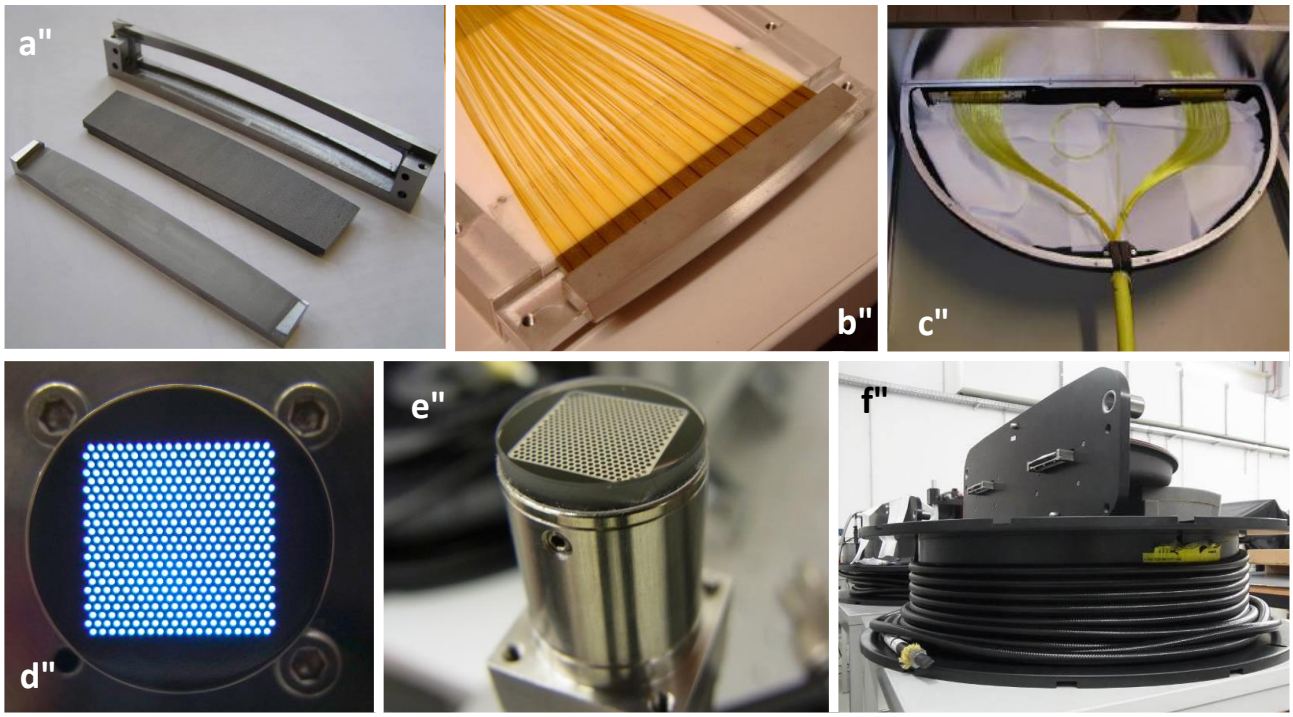

Figure 6. Production of IFU cables at AIP. (a) precision slit assembly components; (b) a slit block with 224 fibers; (c) an integrated output slit assembly with two slit blocks mounted and the fan-out of fibers from the conduit; (d) an input head, back illuminated, with 448 fibers – note the 1/3 fill-factor of the fiber cores; (e) input head with cover lens installed; (f) a completed IFU of 22 m length on transport spool.

The conduit housing the fiber cables underwent extensive design evaluation and prototyping. It is important that the fiber not piston significantly in and out of the conduit where it exits the cable into the slit box. Such pistoning might occur with changes in axial load or ambient temperature swings, and we were particularly concerned about shipping and handling during installation and avoiding twists. We also wished to minimize the weight of the conduit, which can dominate the total weight, and adopted a custom fully interlocked aluminum conduit with PVC sheathing supplied by Hagitec. The ID is 13 mm. As with our previous cables we have an inner sock of Kevlar to protect the fiber from the internal structure of the conduit. In order to stabilize the length of the conduit we tension this inner sock at assembly so that the conduit is somewhat compressed and the resultant spring constant is high. The Kevlar sock has a minimum diameter chosen so as not to constrict the fiber, but still fit in the ID of the conduit. The Kevlar is tensioned during assembly, which stabilizes the length of the conduit assembly and prevents fibers "pumping" in and out and developing torsional stress. We took this design through the full range of motions expected at HET before production and did not see any sign of the fiber pistoning in and out of the conduit at its exit. This has now been borne out by experience with deployed IFUs at the HET.

While many years of use on the Mitchell Spectrograph provided information on the durability of IFU cables, we also conducted a more controlled test in order to uncover any design issues related to durability in the production IFUs before committing to full production. In particular, we first wanted to understand how the fibers behave while in motion, and that might depends on the rate of fiber motion. Second, we wished to monitor how the properties of a VIRUS fiber bundle change due to the accumulation of wear. In order to explore these questions we simulated 10.2 years of wear (188.7 km of linear travel) on a single fiber bundle. The simulated motion was carried out between February and May 2011 on test rig designed and built for this purpose. Results of the lifetime test are described in Ref. 48, and qualified the cable design for final manufacture.

In production, we provided the manufacturers with kits of parts (fiber, mechanical parts, conduit, etc.) and they do the assembly and polishing of the ends. Final integration of the slit blocks into the output slit assembly is done at AIP. We established three production lines, based on qualification work at several vendors. One at AIP, and the others at CeramOptec and FiberWare. Each has been capable of producing at least one IFU per month. Acceptance test and evaluation facilities were set up at AIP. These include microscope examination of polish of the input and output ends against fiducial standards, FRD testing, throughput testing, and fiber mapping and position measurement. A final system

test is performed on each cable with a fiducial spectrograph (one of the First Article VIRUS units), generating a report and metadata that will be used by the reduction software and in record keeping. This report is generated by a lab version of the Cure data reduction package, called "LabCure" (see below).

At the time of writing, 75 of the 78 IFUs for VIRUS have been manufactured, 52 are fully assembled, and 39 have been delivered to the HET. Of these, 16 are deployed on sky.

3.6 Sofware Development

One place where the parallelized nature of VIRUS is a huge advantage is in data reduction software development. Many instruments have suffered from the late arrival of reduction software or from unexpected instrumental features that require the development of new software methods to account for them. Since the VIRUS units will be very close to identical, and very similar to the Mitchell Spectrograph, we have had the advantage of having a full test-bed for the software in operation for several years.

The software for VIRUS must process a highly parallel data stream, quickly, and detect single-line objects, reliably. Development of the final software pipeline for reduction of VIRUS data is being led by MPE. Since VIRUS is naturally a parallel instrument, all the requirements for and attributes of the software have been developed and tested on the prototype. This was a key motivation for the deployment of the Mitchell Spectrograph on the telescope early in the project. Two pipelines have been developed, one in Texas called VACCINE[29] and the other in Munich, called Cure[49,50]. VACCINE was used primarily to reduce and analyze data from the pilot survey on the McDonald 2.7 m, while the algorithms of Cure are tuned for use on the HET. The difference is driven primarily by the plate scale difference between the telescopes. On the 2.7 m, the fibers are significantly larger than the image size, while on HET they are comparable. This leads to differences in the detection algorithm, but not the data reduction methods. Care is being taken to propagate errors and avoid interpolation through resampling of data, which leads to position-dependent smoothing and can alter the noise characteristics. Cure uses a Bayesian detection algorithm that assigns a likelihood of a source to every (spatial and spectral) resolution element. Tests show robust rejection of cosmic rays and reliable detection of 5-σ line-flux objects, as required for HETDEX. The stability requirements for the instrument are driven by the need to know the statistical weight of each pixel, particularly in the spatial dimension, across the fiber profiles, where small movement of the image on the detector can change the weights greatly. We have also demonstrated sky subtraction to the Poisson noise limit, with both pipelines, aided by the fact that most of the fibers of VIRUS are observing sky in any exposure.

We have exploited the advantage to having the ability to exercise software on real data early in the project, and we are now obtaining sky data with 16 units deployed at HET (see below). This is a key advantage of a highly replicated and hence parallel instrument, particularly since such instruments by definition generate large volumes of data. Software must follow a mass-production model as well.

Data are copied automatically to the Texas Advanced Computing Center in Austin where Cure is installed on the Maverick supercomputer. At HET we run the VIRUS Health Check (VHC) a Python utility that acts as quality control for the data as it comes off the telescope and raises flags should there be unexpected data properties. The Resident Astronomers have access to the Python-based VIRUS Data Analysis Tool that presents the data through a simple GUI and allows the data of any IFU to be inspected, analyzed, and even reduced. VHC and VDAT utilize the same libraries as Cure and so have access to all functionality. VDAT manages the complex data accounting necessary with so many instruments. The other key tools at HET are the Observing Conditions Decision (OCD) tool, which manages the HETDEX observations and flags if the conditions are not within requirements, and the Plan and Shuffle tools that select the next targets and provide the setup for the telescope and guiding system. OCD manages the handshake between the telescope and Plan/Shuffle and will evolve into a semi-automatic system able to execute several HETDEX observations in sequence with minimal human interaction.

4. VIRUS ALIGNMENT AND CHARACTERIZATION

Following assembly of collimator units at TAMU and cameras at UT Austin, the spectrographs are integrated at UT Austin and aligned. The alignment procedure involves attaching an adjustment back to the camera cryostat, in pace of the regular back, that incorporates ferrofuidic vacuum feed-throughs for adjustment and locking of the camera mirrors. We also allow small adjustments of the collimator position, which comes pre-aligned from TAMU at the 0.1 mm level. Experience with aligning VIRUS-P highlighted the likely bottle-neck of this step in the large-scale production and led us to develop a deterministic alignment procedure that utilizes moment-based wavefront sensing (MWFS) analysis[51-53]. This moment-based wavefront sensing (MWFS) method relies on the geometric relation between the image shape moments and the

geometric wavefront modal coefficients. The MWFS method allows a non-iterative determination of the modal coefficients from focus-modulated images at arbitrary spatial resolutions. The determination of image moments is a direct extension of routine centroid and image size calculation, making its implementation easy in the alignment of real systems like VIRUS.

The alignment procedure is as follows: using Hg+Cd lamps as the line source, we move the collimator mirror along the optical axis by adjusting three manual micrometers on the back of the mirror taking exposures at five modulations (positions) per run. The IFU input is masked so that the images of the fibers do not overlap on the detector. The acquired images are then processed through the MWFS pipeline software, where the modal coefficients associated with individual fiber images and their errors are estimated. Each estimated coefficient is then fitted by a quadratic curve across the slit or the wavelength dimension, resulting in the gradients of the coefficient in both directions across the CCD. The gradients are then used to determine the required tip and tilt angles of the camera mirror and/or the collimator mirror. The software predicts the required move for both optics to achieve alignment. We restrict the motion of the collimator since the optics come pre-aligned to a certain level from TAMU and there is some degeneracy between camera and collimator moves. For the defocus term, the zero-th order curve fit value provides the overall piston focus correction. We use the piston focus estimate only as a guidance and do not attempt to completely zero out the focus term because the zero defocus in fact results in slightly larger PSF. Therefore, the final focus adjustment is done by a combination of the visual inspection of the fiber images and then confirmed by the final contrast test.

Throughout the alignment of the VIRUS units so far (50 units), we typically needed two modulation runs and thus two rounds of corrections. After these corrections, we fine-tune the focus by the contrast test on the fully exposed IFU images without the IFU mask. In the contrast test, we slice through the centers of the fully exposed fiber images in the slit dimension and then compute the peak value of each fiber image and the valley value of between two fibers. The requirement that the valley be lower than 50 percent of the peak is the root requirement of the error budget for the optical fabrication and alignment. We compute the standard contrast of (Ipeak −Ivalley)/(Ipeak +Ivalley) for each fiber image. The requirement is that 90 percent of the fiber images across the CCD must have the contrast value higher than 60 percent (equivalent to a cross over point of 25% of the peak). This requirement is much tighter than the original 50% cross-over point requirement that we established in tolerancing the optical design for production, reflecting the power of this method to greatly exceed our requirements by making the alignment error contribution to the image sizes quite negligible. The image quality performance of every VIRUS production unit has exceeded that of VIRUS-P by a substantial margin. The contrast test gives a quite sensitive feedback on the focus adjustment.

While the analysis underlying the MWFS technique is fairly complex, we have scripted the alignment scheme and have been able to train non-expert users to achieve results that are exact and deterministic. This situation contrasts with the very inexact process usually employed to measure image size over the detector and make incremental adjustments to minimize it, as was employed on VIRUS-P. The time required for the alignment is roughly half a day per channel plus time to pump the cryostat and cool the detectors. We have achieved a steady state of 2 units (4 channels) per week.

Following alignment, VIRUS units undergo a characterization[36] before being packed for storage and eventual transport to the HET[5]. The characterization station is located in a separate lab that can be darkened sufficiently to ensure no stray light for the tests. A lab calibration unit houses a laser driven light source (LDLS, see below) for flat-fielding and Hg+Cd line lamps for wavelength determination. A standard production IFU is designated for these tests so there is a uniform reference. In addition, a "pixelflat" head that mounts in place of the IFU head and provides a continuous illumination of the two slits rather than the highly modulated IFU output is utilized to provide the source for pixel-flat-fields of the detector, free of the spatial dimension fiber modulation. This is important for generating maps of the pixel-to-pixel QE variations and to identify bad pixels. Bias levels are set and photon transfer curves are generated to confirm read noise and gain of each channel. Sets of bias and dark frames are recorded to act as a reference once the units are installed at HET. Python scripts provide automated characterization datasets in conjunction with the VDAS control system and a lab version of the Cure data reduction package has been developed to provide a digest of the results for reports on each unit. The metadata generated by the characterization step travels with the units to the mountain and will be part of the data delivery when in use. Full details of the characterization and results from the first 16 units deployed at HET are presented in Ref. 36, and Fig. 7 from that reference shows results of fiber to fiber throughput for 15 units compared between lab and sky.

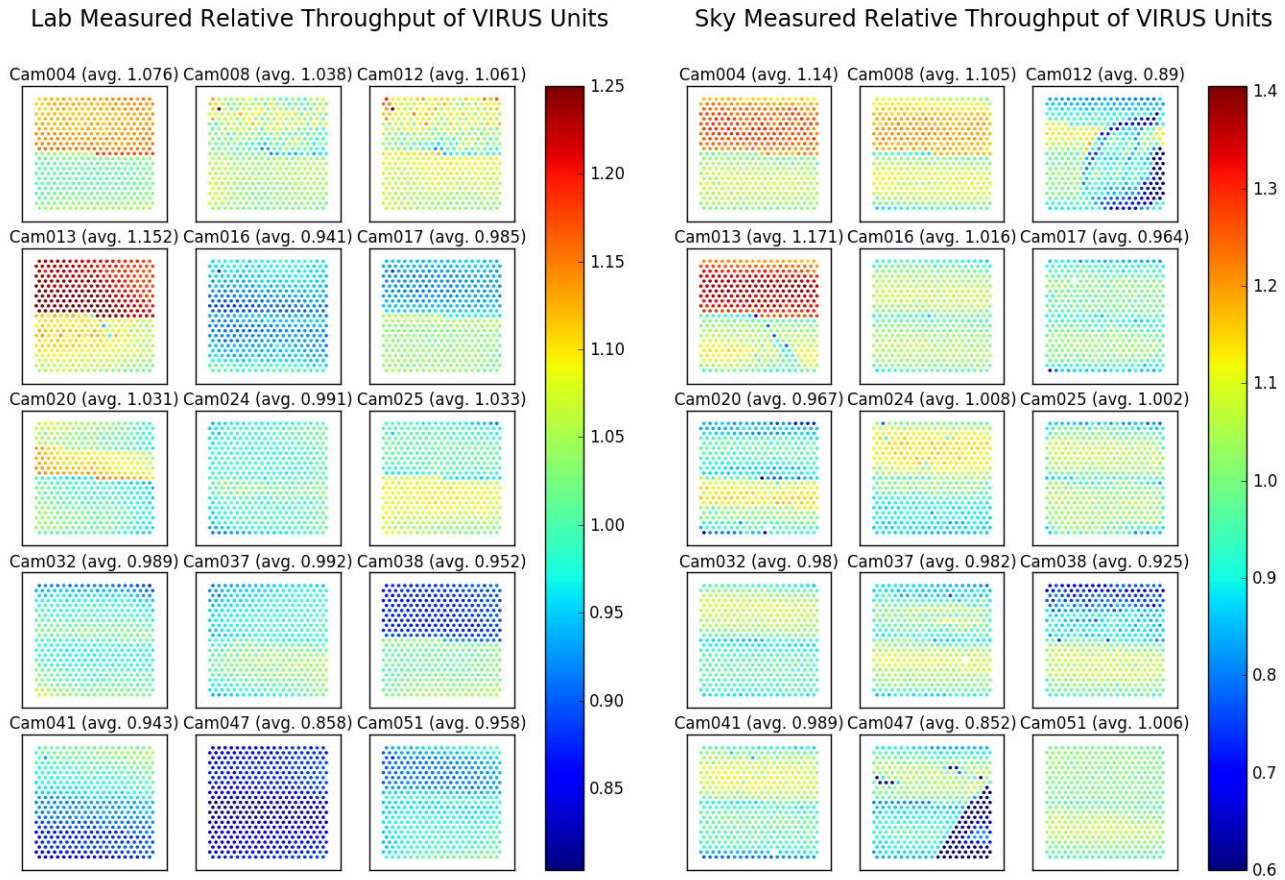

Figure 7. Comparison of characterization data obtained in the lab (left) with data obtained on sky during twilight (right) for 15 VIRUS units. Data in the lab is obtained with the same reference IFU and at HET each unit has a different IFU. The sky data are obtained simultaneously, while the lab data are referenced to the LDLS, which has output stable to a few percent. Note two damaged IFU cover lenses are evident in the sky data. The two channels of the spectrograph units map to upper and lower halves of the fiber matrix as can be seen from some discontinuities in throughput. See Ref. 36 for details.

5. VIRUS INFRASTRUCTURE ON HET

The VIRUS spectrograph units take up a large volume and require a distributed liquid nitrogen (LN) cooling system[44,45]. The infrastructure to support VIRUS is a significant undertaking and is being integrated with the deployment of the WFU. Since the wavelength coverage of VIRUS extends down to 350 nm, the average fiber length had to be minimized commensurate with keeping the mass of the instrument off the telescope structure and providing sufficient access to the primary mirror and tracker with the HET man-lifts and crane. Following extensive optimization and evaluation by HET staff, we settled on a configuration with VIRUS units housed in two large enclosures flanking the telescope structure and riding on a separate air-bearing system during rotation of the telescope in azimuth (Fig. 1).

VIRUS units and the new LRS2 low-resolution spectrograph are housed in the large enclosures mounted on each side of the telescope (Fig. 8(a)). They are supported by the VIRUS support structure (VSS) framework designed to carry the weight of the enclosures and spectrographs without connecting to the main structure of the telescope in order to ensure no coupling of wind-shake-induced motion into the tracking of the telescope. For changes in azimuth, the VSS rides on its own set of air bearings and is dragged by the main structure drives through loose linkages. When the structure is placed down, there is no significant coupling between the structures except through the concrete ring-wall pier at the base.

The two large VIRUS enclosures are mounted to the VSS and are essentially sealed clean-rooms with a heat removal system to avoid degradation of the seeing by the heat generated by the detector controllers and electronics from

escaping to the dome by convection or air leaks. They are based on large steel space-frames which TAMU outfitted with skins and removable hatches to provide access to both sides of the spectrograph for camera maintenance and IFU access, respectively[54].

The heat removal system is separate for each enclosure. It uses facility glycol as the primary coolant fluid with a 600 W "Thermocube" thermoelectric cooler on each side providing the ability to tune the temperature of the circulating air to keep the overall environment close to ambient temperature at night. During the day we attempt to keep the enclosure temperature close to nighttime temperatures. Heat removal is needed to keep the VIRUS detector controllers from overheating and to remove the heat they generate so it does not enter the dome and degrade the seeing environment. Air is drawn through the controllers by the system and cold HEPA-filtered air is returned at the top of each sealed enclosure[54]. Metrology systems within each enclosure, run from a custom PLC system, monitor the environment and performance of the system.

The distributed and large-scale layout of the VIRUS array presents a significant challenge for the cryogenic design. Allowing 50 W heat load for each detector, with all losses accounted for and a 50% margin, the cooling source is required to deliver 3,600W of cooling power. We engaged the late George Mulholand of Applied Cryogenics Technology to evaluate the options and provide an initial design[44]. Following a trade-off between cryocoolers, small pulse-tubes and liquid nitrogen based systems, it is clear that from a reliability and cost point of view liquid nitrogen is the best choice. The problem of distributing the coolant to the distributed suite of spectrographs is overcome with a gravity siphon system fed by a large external dewar. A trade-off between in-situ generation of the LN in an on-site liquefaction plant, and delivery by tanker has been made, with the result that the delivery option is both cheaper and more reliable[44].

An important aspect of the cryogenic design is the requirement to be able to remove a camera cryostat from the system for service, without impacting the other units. This is particularly difficult in a liquid distribution system. A design has been developed that combines a standard flexible stainless steel vacuum jacketed line (SuperFlex) to a cryogenic bayonet incorporating copper thermal connector contacts into each side of the bayonet[44,45]. When the bayonet halves are brought together they close the thermal contact. The resulting system is completely closed, i.e., it is externally dry with no liquid nitrogen exposure. The camera end of the connector is connected by a copper cold finger to the detector. Each spectrograph unit has its own SuperFlex line which we term the "dogleg", removing heat to cool the two CCDs. This design has another desirable feature: in normal operation the SuperFlex tube slopes downwards and the bayonet is oriented vertically. Liquid evaporation will flow monotonically up in order to avoid a vapor lock. If the bayonet is unscrewed and raised upwards, a vapor lock will occur and the bayonet will be cut off from the cooling capacity of the liquid nitrogen. This effectively acts as a "gravity switch", which passively turns off cooling to that camera position. We run the CCDs at about -110 C, controlled via heating resistors and a control loop based on an RTD sensor. The performance of the bayonet is not changed when the connection is broken and remade.

The contract for the fabrication of the VCS was awarded to Midwest Cryogenics and the 11,000-gallon vacuum jacketed holding dewar is supplied by Praxair as part of the contract for the cryogen supply. It was delivered in October 2014 (Fig. 8) and when in full operation will have in excess of 4 weeks operation capacity and a 6,000 gallon delivery of LN will be required every two to three weeks. The enclosures and VCS were installed in February 2015 and immediately passed the first cool down test. Site acceptance of the VCS was at the end of March 2015.

In addition to the supply-side of the VCS, we have deployed the VIRUS Cryogenic Safety System (VCSS). The requirements for the VCSS are to protect personnel and equipment in case of malfunction of the VCS or leaks of the LN lines. We use sensitive oxygen sensors throughput the facility as well as monitoring the liquid flow rate and the liquid level in the header tanks atop each enclosure. Abnormalities trigger valve closures and alarms. We currently run one side of the VCS and have gained valuable experience as we have brought the VCSS on line. The system has self-monitoring and emergency notification by visible and audible alarms and by dialing preset phone numbers.

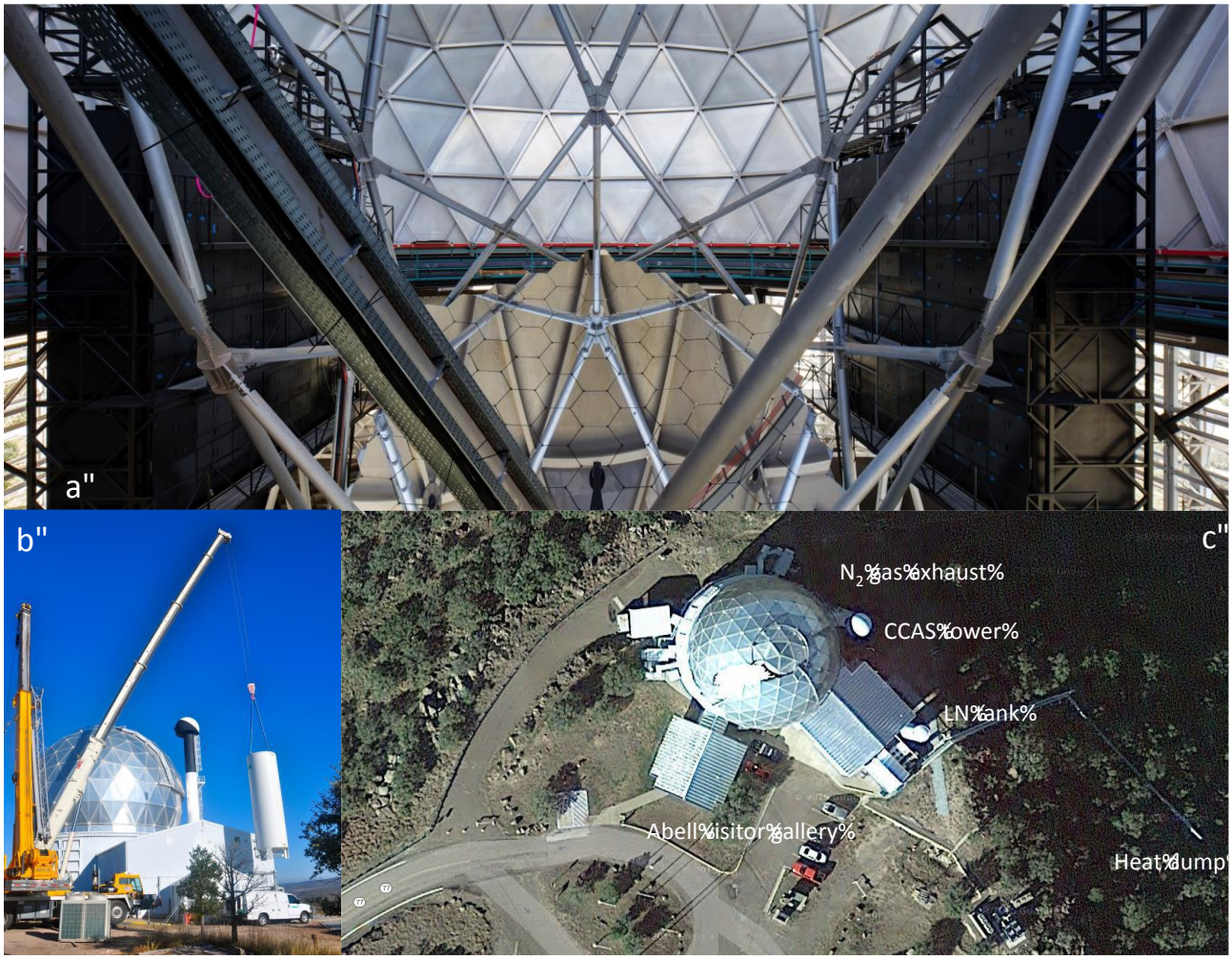

Figure 8: VIRUS infrastructure (a) view of the HET from the front showing the primary mirror and the large VIRUS enclosures either side of the telescope structure. The phase separator tanks of the VIRUS Cryogenic System can be seen mounted to the top of each enclosure; (b) 11,000 gallon liquid nitrogen (LN) tank to supply VIRUS cryogenic needs being lifted into place at the HET; (c) Google satellite view of HET showing that the support infrastructure is visible from space.

6. VIRUS EARLY DEPLOYMENT

At the time of writing we have deployed 16 VIRUS units and IFUs on HET, along with the two units of the new low-resolution spectrograph (LRS2-B and LRS2-R[25,26]) that also utilize the VIRUS cryogenic, enclosure, and readout infrastructure. This microcosm (20%) of the system allows us to test the cryogenic and readout infrastructure fully and start training of HET personnel in the maintenance of the system. It also allows instrument commissioning to start and provides a flow of data to begin testing of the data processing and quality control. Such a staged deployment is an enormous advantage of a replicated instrument like VIRUS. By the time the majority of the units are installed we will have many months experience with the system and should be able to commence the HETDEX survey even before the last units are installed.

6.1 Hardware deployment

Figure 9: VIRUS spectrograph unit deployment; (a) 8 units staged for installation in HET receiving bay; (b) VIRUS unit rigged and balanced for lifting with HET dome crane; (c) 8 units installed in one of the VIRUS enclosures, prior to installation of enclosure covers.

Deployment of the IFUs and VIRUS units occurred in separate phases, with the IFUs going in first (Figs. 9 and 10). Careful planning resulted in quite rapid deployment, but naturally led to refinements of the procedures that will be applied to future deployments. Two steel cables either side of the tracker, hung from a strain relief on the PFIP set the route of the IFUs between the tracker and the enclosures. We are very careful not to twist the IFU fiber cables since this can result in stress of the fibers in the corners of the input matrix, as seen with the VIRUS prototype. At AIP, following characterization, the cables are wound onto plastic spools of about 1 m diameter with the input head being spooled first so that the bulky tailpiece can be handled more easily during packing for shipment. Four IFUs are packed in each crate and 2-4 crates are shipped at once from Germany to HET. After unpacking an inspection, when ready for deployment, the IFU is wound onto a spare spool such that the input head is ready to be unspooled first. The jig for this re-spooling holds the IFU spools in a horizontal aspect with the tailpiece sitting on top of the spool. When ready for deployment, the IFU is lifted to the top of the appropriate enclosure, where two people handle its unspooling, and placed on a hub in a horizontal aspect. One person guides the input head end to the team in the cherry-picker that maneuvers the IFU cable to the HET tracker, while the other insures that the cable remains spooled and is unwound in a controlled manner. A further person stationed on the service platform of the tracker takes care of the routing over the strain relief and the installation of the head in the input head mount plate (IHMP). Once the cable is routed, it is secured to the rest of the cables and to the steel cable at multiple points with straps. Finally, each input head is secured to the IHMP with small screws from the underside. This is done at one time for all the deployed IFUs, since removing and handling the IHMP assembly is time consuming, and it needs to be mounted on the telescope during IFU deployment to insure that the lengths are correct.

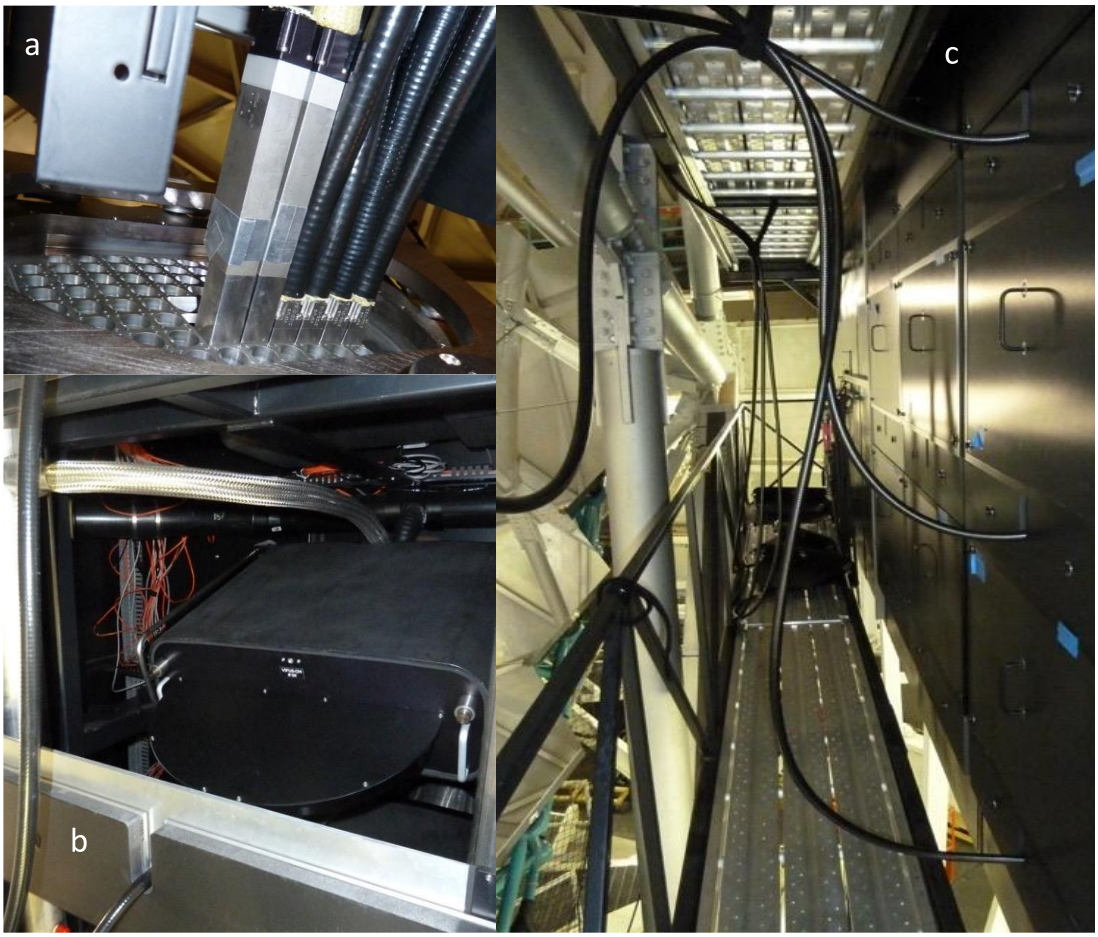

Figure 10: VIRUS IFU deployment (a) 16 VIRUS IFUs (black conduit) and the two LRS2 IFUs installed in the input head mount plate (IHMP) at the prime focus of the HET; (b) IFU tailpiece installed on a VIRUS unit in the enclosure, note the stainless steel braid on the liquid nitrogen "dogleg" cooling the spectrographs; (c) VIRUS enclosure sealed up after IFU installation.

Spectrograph units were deployed in batches of 8 units. We found that 8 can be deployed comfortably in a workweek, including transport and testing/documentation, and having a day contingency. VIRUS units are designed to be handled by two people and 8 can easily be transported in rented vans, a further advantage of the modular nature of the instrument. The most time-consuming step is pumping the vacuums of the cryostats and Figure 9(a) shows 8 units staged in the HET receiving bay undergoing pumping. By having several vacuum pumps running, we are able to prepare and deploy 8 units in a day. The sequence for each unit following vacuum pumping involves rigging and lifting by the dome crane (Fig 9(b)), insertion into the appropriate enclosure slot, and then cooling as quickly as possible to ensure a good vacuum. As described above, cooling is provided by a metal-to-metal bayonet connection, and as soon as it is oriented correctly and tightened, liquid nitrogen flows down the vacuum jacketed "dogleg" to the heat exchanger tip and the system begins to cool. Before cooling, the detector readout system is brought up and we insure that we can read temperatures so that the process can be monitored. Occasionally the position of the unit has to be adjusted slightly to insure that there is a monotonic curve to the "dogleg" without any high points that could trap nitrogen gas and impede the flow of liquid to the tip. This situation is evidenced by the temperature stalling at a few degrees below freezing. Usually the temperature of the cryopump goes down rapidly to -150 C, after which the system can be left to cool without monitoring. This process can be repeated for 8 units in a day (Fig 9(c)).

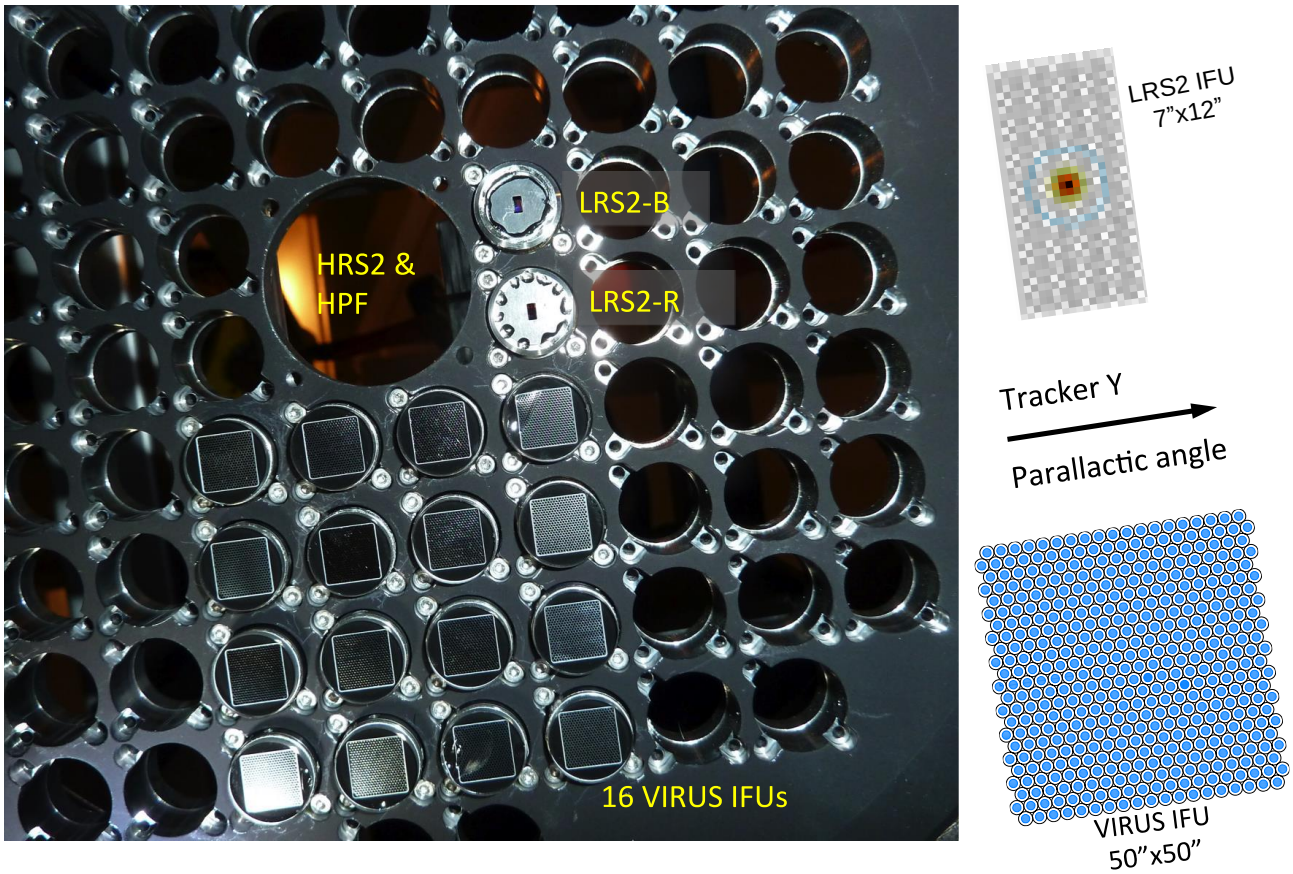

Figure 11: Populated focus of HET with VIRUS and LRS2 IFUs mounted in the precision machined input head mount plate (IHMP). The 16 VIRUS IFUs are arrayed in a 4x4 grid, sampling the full radial extent of the science field of view. The LRS2 IFUs for the LRS2-B and LRS2-R units are coupled by microlens focal reducers that proved full fill factor over a smaller field of view. The central position is reserved for future high resolution spectrographs and a bore-sight imager that allows the IHMP and the acquisition camera fields to be tied together by observing stars at the center of the field of view.

Before mounting on the spectrograph unit, each IFU is inspected for any stress that might have been created in the tailpiece, by removing the inspection cover to look at the fibers going to the slit blocks. Adjustments can be made to the conduit clamp in the tailpiece, if needed (which is rare). The tailpiece is then mounted to the kinematic mounts on the spectrograph unit and the enclosure sealed up. Figure10 shows several views of the process.

Figure11 shows the “photons-eye” view of the deployed IFUs for VIRUS and LRS2. The direction of the parallactic angle, which is the vertical axis of the tracker beam of the HET is shown for reference. The parallactic angle on the sky depends on the telescope azimuth, so on the target declination and whether the track is east or west. Also shown in the figure are the orientations of the IFUs for LRS2 and VIRUS. LRS2 has fully-filled lenslet coupling and hence has smaller area than VIRUS[27].

6.2 Instrument Commissioning

The basic behavior of the VIRUS units was established using the Facility Calibration Unit (FCU), which injects flat field and emission line source light into the entrance of the WFC and mimics the ray bundles propagating through the optical system. For VIRUS we use a Laser Driven Light Source with a laser pumped Xenon plasma (LDLS[§]) for flat fielding to provide adequate UV light and Hg and Cd emission line lamps. Properties of the spectrographs were compared with baseline lab data taken during the characterization phase (see above). While each IFU plus spectrograph units had not been tested together before, we find a good correlation between performance in lab and on the telescope, indicating that we can

[§] Model EQ-99X-FC-S from Energetiq

align the IFUs and spectrographs separately against fiducial units and achieve our requirements when they are combined finally at the telescope.

As part of bringing the system on line, a python script allows various combinations of calibration data to be taken with the CAMRA/VDAS system interacting with the FCU through the TCS. This script is run each night to obtain standard sets of calibration data (flats, arc lamps, bias, darks), along with twilight flats that provide a baseline calibration. A short version is used each afternoon to check the health of the system during overlap between the day and night staff. As such, we are well on the way to developing the final operations model for the full VIRUS instrument, based on experience with the early deployment microcosm.

The basic instrument properties tested and systems developed during instrument commissioning are:

- Alignment and stability of deployed spectrographs
- Detector noise characteristics when run as a distributed system in the enclosures
- Demonstration of parfocality of the instrument with the acquisition camera (ACAM) and the guide probes (GP)
- Establishing the centers, plate scales, and orientation of each IFU on sky in relation to the telescope coordinate system
- Measuring the image quality delivered by the HET over the full radial extent of the field (in combination with ACAM and GP measurements obtained simultaneously)
- Demonstrating that the differential atmospheric refraction (DAR) is detected and follows the simple function predicted by atmospheric conditions, the elevation of the site, and the zenith distance of the HET (which is close to fixed at 1.22 airmasses at center track)
- Measuring the orientation of the ACAM and GP systems with respect to the IHMP frame of reference measured by the IFUs. Once this has been established, the rotational offset to align the system to the parallactic angle can be made. These measurements also allow the object acquisition tools to be set up so that the ACAM and GP positions are referenced to the IFU positions for LRS2 and VIRUS
- Observing spectrophotometric standards to measure throughput and verify the illumination function of the HET with field angle and tracker position

The spectrograph units all exhibit image quality and stability as predicted from lab measurements. The detector system has noise in line with the best seen in the lab in Austin, and there is no sign of noise pickup or any cross-talk between channels.

Observations of globular clusters (GC) proved to be particularly important in these tests. Figure 12 shows a setup on M3. Since there are hundreds of stars detected by 16 VIRUS units in each observation, and their positions are known with high accuracy, the 1/3 fill factor of the IFU fibers does not matter in deriving the astrometry and image quality, and repeat observations allow great precision in deriving the positions and orientation of the IFUs. We have demonstrated that the positions are as intended to about 0.1 arcsec precision, which is the measurement error of the observations. The IHMP is machined to tolerances below 0.05 arcsec projected on sky.

Since the VIRUS units provide the only measurements over the full science field of the upgraded HET, these observations have also proven important in verifying HET performance, particularly image quality. Detailed wavefront measurements over the science field were obtained with small deployable WFS that mount in the same seats as the IFUs and hence tie together the physical and optical focal surfaces of the telescope. These measurements vindicated the alignment of the WFC and showed that the system meets image quality specifications. See Ref. 16 for details of this process. VIRUS observations have confirmed that the image quality is almost independent of field angle, and tie together images obtained with the ACAM and the GPs. We have been able to measure the DAR with high precision from GC data, and can fit the smooth curve with a single free parameter. We chose not to have an atmospheric dispersion compensator for VIRUS because even a complicated optic would have residuals from the compensation that would be difficult to model. We can easily model the DAR in the VIRUS data from the data themselves and a simple model, so we can correct positions to a fiducial wavelength of 550 nm. This is a particular advantage of IFU instruments, which can follow the DAR and gather all the light independent of wavelength.

Once the frames of reference for the IHMP, ACAM and GP assembly were tied together using GC data, we could deploy object acquisition tools that set up the telescope based on desired targets on specific IFUs. The first version of this tool ("Gstar") was developed by the HET nightstaff and proof of performance then allowed us to start using the HETDEX setup tool called "Shuffle". An example of a Shuffle setup on GC M3 is shown in Fig 12, overlaid on a color-composite image from SDSS. The patrol regions of the two GPs and two WFS are shown in the outer annulus along with the positions

of the VIRUS IFUs and the parallactic angle of the observation. Guidestars and WFS stars are selected, and the output sent to the TCS to command the probes to position and also produce an expected image of the ACAM field for the particular pointing. On the ACAM image, coordinates of stars in the field are noted, so that the telescope operator simply needs to place the appropriate star on the ACAM in order for the pointing to be secure. The result of this methodology is that the setup stars are always bright even if the target object is invisible (or in the case of VIRUS not within the 3 arcminute field of view accessible to the ACAM). Gstar or Shuffle can be run ahead of time or while the previous object is being observed, and the observation queued up when ready. The process is sufficiently fast that overheads are small, and we achieve setups of 5-7 arcminutes dependent on the length of azimuth move, even on blind objects.

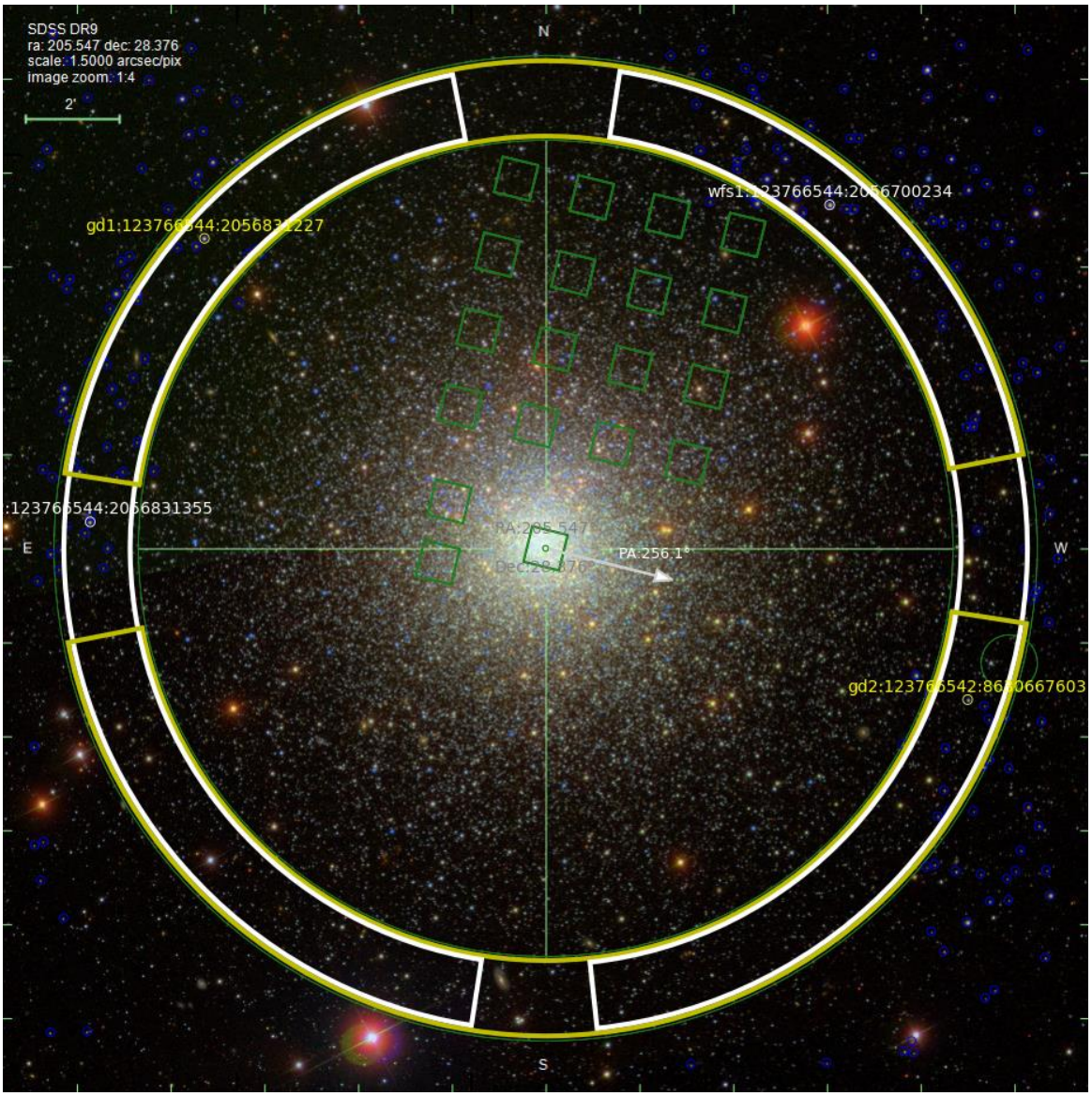

Figure 12: Example setup of HET using the "Shuffle" software tool. The outer annulus extends from 9-11 arcminutes field radius and has the patrol regions of the two guideprobes and 2 wavefront sensors indicated, along with the identifications of the guide and wavefront stars chosen by the software. The parallactic angle direction is indicated by "PA" and an arrow. This is the direction of the zenith for this particular observation, and sets the orientation of the IFU pattern on the sky.

6.3 Early science Commissioning

An important goal of the early deployment of VIRUS is to test the full system including the data reduction pipeline. Cure, on real data. We interleaved instrument commissioning work with observations of key fields such as the Goods-N and the

Extended Groth Strip region from the Candels project[55]. These regions have hundreds of redshifts measured and we could expect to compare emission line objects detected in VIRUS data with known properties.

Figure 13 shows an example of data on M3 from 16 units reduced with Cure and presented as images summed over the spectral dimension (350-550 nm). The observation was identical to those planned for HETDEX, consisting of three exposures, each of 6 minute duration, with the IHMP position dithered between exposures to fill in the coverage of the IFU fiber pattern on sky. In comparison with images from SDSS, the depth of the summed images is very similar to, and reaches AB~23, and they exhibit very similar image quality of around 1.6 arcsec FWHM. Such data have been the basis for many of the commissioning observations discussed above. Note that a few instrumental features remain in these data including cracked input lenses on two of the IFUs. Three amplifiers exhibit poor serial transfer efficiency and three CCDs show elevated background due to spurious noise. The universal timing file for the deployed system is being adjusted to see if these features can be eliminated.

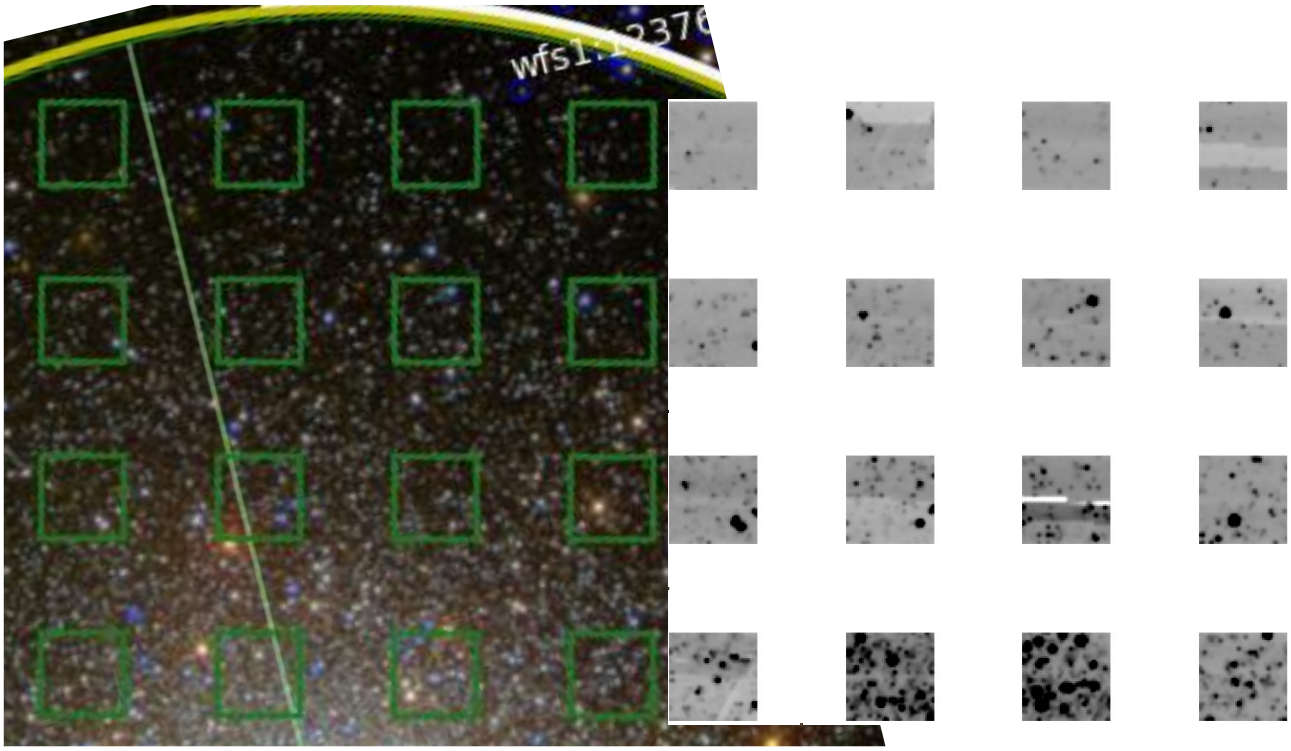

Figure 13: Example of reduced data from the 16 deployed VIRUS units employing more than 7000 fibers. Left shows a zoom-in on the Shuffle setup for the M3 gobular cluster, overlaid on the SDSS color-composite image. Right shows the VIRUS data collapsed in the wavelength dimension to produce an image from 350-550 nm. All objects detected in the SDSS image are seen in the corresponding VIRUS data, which exhibits similar image size as the SDSS imaging data. The 4x4 matrix of IFUs covers 8.2 arcmin on the diagonal. The IFUs are each 50x50 arcsec^2 area (11 sq arcmin in total) and are mounted on 100 arcsec centers.

Even the limited observations of GOODS-N and EGS have yielded hundreds of emission line identifications, which are being compared with known objects in these well-studied fields. Fig. 14 shows examples of a LAE and an [OII] emitter. These data are being used to test the basic function of the detection algorithms and compare sensitivity with expectations. Early indications are that the system is reaching a depth that is in line with expectations, but more work is needed to quantify the throughput and sensitivity.

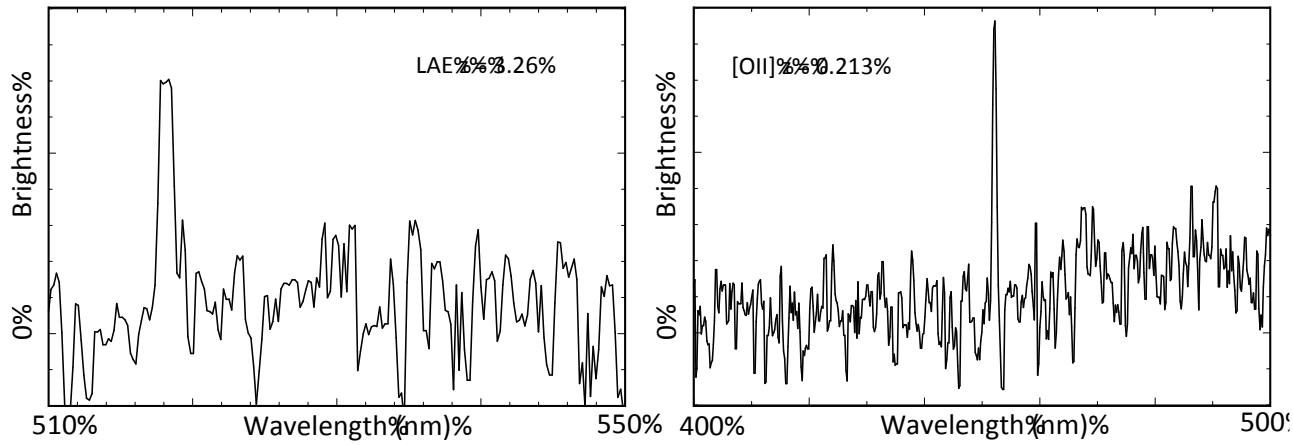

Figure 14: Examples of extragalactic emission line sources detected in early science commissioning data obtained on the Extended Groth Strip (EGS). Left is a Lyman-α emitting galaxy at z=3.26 and right is a lower redshift [OII] emitting galaxy. The [OII] emitter has clearly detected continuum emission in addition to the emission line. These objects are already known from extensive spectroscopy on the EGS, allowing us to gauge the sensitivity of VIRUS.

Instrument and science commissioning will extend through the rest of 2016 as more VIRUS units are deployed and we bring the remaining aspects such as data quality control into the system. During the fall we will observe fields within the HETDEX/SHELA equatorial strip that has ancillary imaging data at wavelengths from the ultraviolet to sub-mm. Those data will allow projects on galaxy evolution within the context of environment to be undertaken well before the dataset becomes large enough to address questions in dark energy. HETDEX detects star forming galaxies and AGN at the epoch of the peak of activity in the history of the universe and allows galaxy properties to be placed in the context of the large-scale structure that will be traced by the LAEs.

We expect to commence the HETDEX survey once 50 units are deployed and the first season will be on the spring field in 2017. The final VIRUS units will be deployed by mid 2017. After that, a three year survey will be undertaken utilizing most of the dark time on the HET to address questions of the evolution of dark energy, the curvature of the universe, and the growth of structure, among many others.

7. THE VIRUS FUTURE

VIRUS was designed from the outset to allow exchange of gratings to change wavelength ranges and resolutions, and the Mitchell Spectrograph is used on the McDonald 2.7 m Smith Telescope with four different VPH gratings. Due to the large size of the fibers projected on the sky, it is very sensitive for low surface brightness extended features, for which the sensitivity surpasses that of instruments on the largest telescopes. In addition to this flexibility and sensitivity, the generic nature and massively replicable characteristic of the instrument can allow us to adapt the VIRUS concept to a wide range of not only telescope diameters (1m ~ 40m), but also observing modes (single to multiple objects), in a very cost-effective manner. On small telescopes, a single IFU can cover very large fields of view with large spatial elements ideal for studying resolved galaxies, while on large telescopes the same IFU can observe single objects in varying image quality, while obtaining a simultaneous background observation.

Replicable spectrographs like VIRUS allow many different slicing modes between field and wavelength coverage/resolution, and these are discussed in Ref. 1. In that review we present Fig 15, which plots grasp (AΩ) against spectral power for survey instruments, and argue that the constraints of detector area and instrument size drive us into the replicated regime for survey instruments on the next generation of ELTs. A highly-replicated spectrograph has not been proposed as a first-light instrument for any of the ELTs. The huge grasp of MUSE[12] and VIRUS makes them quite adaptable to ELTs and certainly the scale of these instruments is "extremely large" (MUSE takes up a whole Nasmyth platform at VLT and VIRUS fills two clean-room enclosures, each 6x6x1.5 m^3). The power of replication is illustrated in Figure 15, following Bershady[56,57] and adapted from Ref. 1, we plot instrument areal grasp (AΩ) versus spectral power (the product of the number of spectral resolution elements and the resolving power $N_\lambda R$, where $R=\lambda/\delta\lambda$ for wavelength λ and spectral resolution δλ) as a useful metric in following the evolution of total instrument grasp (the product of the two quantities)[1].

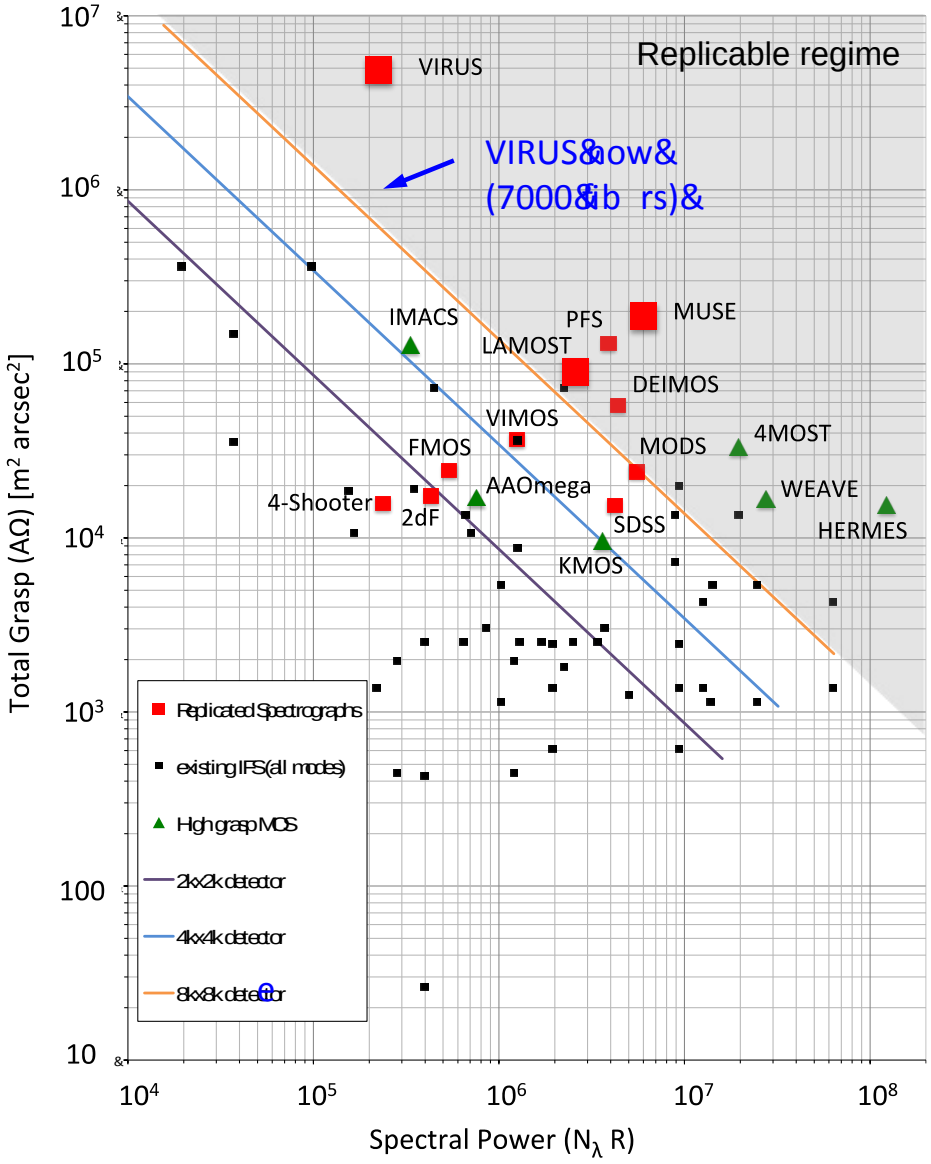

Figure 11. Performance metrics for VIRUS compared with other instruments, both existing and planned, after Ref. 1. Total Grasp is the product of telescope collecting area and area subtended by the sky spatial elements. Spectral Power is the product of the resolving power and the number of spectral resolution elements. Diagonal lines represent the loci of instruments with varying total detector pixel count. The grey shaded region is the zone of replicated instruments, as noted. Integral field spectrographs (IFS), high multiplex multi-object spectrographs (MOS) and replicated spectrographs are compared. The highly replicated instruments are emphasized by larger symbols. The location of the current deployment of 16 VIRUS units is noted. This microcosm of 20% of VIRUS is indicated and already has the highest grasp of any instrument currently deployed.

In Figure 15 we show the locus of these quantities for different-sized detectors, extending up to the maximum current CCD pixel-count (N_{pxl}) used in spectrographs of about 8kx8k pixels (or 6kx12k) achieved on single wafers or small mosaics. The loci for each detector size are plotted for the following instrument parameters: f/1.3 camera focal ratio (a practical limit for refractive optics), 15 μm pixel size typical of modern CCDs used in astronomy, 4.0 pixels per resolution element with a packing efficiency of 65% to allow for separation of spectra on the detector, and resolving power of R=1000 typical of large survey spectrographs on a range of telescope sizes. Fig. 11(left) shows the metric for IF spectrographs, multi-object spectrographs (MOS) and replicated instruments. Replicated instruments are defined as any with more than one copy, but the highly replicated instruments are emphasized with larger symbols. The loci at constant N_{pxl} are diagonal and form parallel lines with increasing N_{pxl}. The loci reflect the fact that the available detector area is divided between

spatial and spectral elements depending on details of instrument design driven by science requirements. Available detector size is a primary driver of the evolution of spectrograph capability. The shaded region of beyond the 8kx8k N_{pxl} locus in Figure 15 is the domain of replicated instruments[1].

It is interesting to consider that the HET is designed for the site seeing at McDonald Observatory and delivers typical images of 1.3 arcsec. As a result, VIRUS is designed with 1.5 arcsec. diameter fibers, to maximize the grasp. The product of image size and telescope diameter for HET is very similar to those of the ELTs with ground layer adaptive optics, so one can regard the HET as the first ELT in regard to the challenges of building instruments for it. Conversely, VIRUS is the ELT-class instrument to be deployed. The locations of the ELT instruments on Fig. 15 indicate why high grasp through replication will become essential to the challenges posed by the ~50 million spatial resolution elements available in an ELT field of view. Of order a percent of the spatial elements will have an object, many of which will be of interest, so taking full advantage of these telescopes will be a significant challenge that replication can begin to address. Many thousands of targets will be available, rather than hundreds. The ability to feed multiple instruments, whether VIRUS-like or not, through an adaptable targeting system like the MANIFEST feed proposed for GMT[58], will also be an important part of any solution.

8. SUMMARY AND STATUS

HETDEX consists of the HET WFU, VIRUS, and the blind spectroscopic survey of 420 sq. degrees. The HET is back on line with the widest field of view of any 10 m telescope and performance significantly improved over its old incarnation. The early deployment of 20% of VIRUS is allowing us to advance all aspects of observing, data handling, and data analysis with a microcosm of the final instrument. It is already the highest grasp instrument in existence. When complete next year, the combination of the 10 m wide-field HET with the grasp of VIRUS, with 35,000 fibers on sky, will create a unique facility that will be able to survey vast areas of sky spectroscopically for the first time.

ACKNOWLEDGMENTS

HETDEX is run by the University of Texas at Austin McDonald Observatory and Department of Astronomy with participation from the Ludwig-Maximilians-Universität München, Max-Planck-Institut für Extraterrestriche-Physik (MPE), Leibniz-Institut für Astrophysik Potsdam (AIP), Texas A&M University, Pennsylvania State University, Institut für Astrophysik Göttingen, University of Oxford and Max-Planck-Institut für Astrophysik (MPA). In addition to Institutional support, HETDEX is funded by the National Science Foundation (grant AST-0926815), the State of Texas, the US Air Force (AFRL FA9451-04-2-0355), by the Texas Norman Hackerman Advanced Research Program under grants 003658-0005-2006 and 003658-0295-2007, and by generous support from private individuals and foundations.

Financial support for innoFSPEC Potsdam of the German BMBF program *Unternehmen Region* (grant no. 03Z2AN11), and of Land Brandenburg, MWFK, is gratefully acknowledged. MMR also acknowledges support by the German BMI program *Wirtschaft trifft Wissenschaft*, grant no. 03WWBB105.

We thank the staffs of McDonald Observatory, HET, AIP, MPE, TAMU, IAG, Oxford University Department of Physics, the University of Texas Center for Electromechanics, and the University of Arizona College of Optical Sciences and Imaging Technology Lab for their contributions to the development of the WFU and VIRUS. Matthew Bershady kindly supplied his compilation of IFS characteristics used in Figure 15. We thank Chris Clemens and Jim Arns for helpful discussions during the development of the gratings for VIRUS, and Roger Smith and Ian McLean, for their assistance in reviewing the VIRUS detector system.

REFERENCES

[1] Hill, G.J., "Replicated spectrographs in astronomy", Advanced Optical Technologies. Vol 3, Issue 3, 265 (2014)
[2] Hill, G.J., MacQueen, P.J., Palunas, P., Kelz, A., Roth, M.M., Gebhardt, K., and Grupp, F., "VIRUS: a hugely replicated integral field spectrograph for HETDEX", New Astronomy Reviews, 50, 378 (2006)
[3] Hill, G.J., MacQueen, P.J., Smith, M.P., Tufts, J.R., Roth, M.M., Kelz, A., Adams, J.J., Drory, N., Barnes, S.I., Blanc, G.A., Murphy, J.D., Gebhardt, K., Altmann, W., Wesley, G.L., Segura, P.R., Good, J.M., Booth, J.A., Bauer, S.-M., Goertz, J.A., Edmonston, R.D., and Wilkinson, C.P., "Design, construction, and performance of VIRUS-P: the prototype of a highly replicated integral-field spectrograph for HET", Proc. SPIE, 7014-257 (2008)

[4] Hill, G.J., Cornell, M.E., DePoy, D.L., Drory, N., Fabricius, M.H., Kelz, A., Lee, H., Marshall, J.L., Murphy, J.D., Prochaska, T., Tuttle, S.E., Vattiat, B.L., Allen, R.D., Blanc, G., Chonis, T.S., Gebhardt, K., Good, J.M., Haynes, D.M., MacQueen, P.J., Rafal, M.D., Roth, M.M., Savage, R.D., and Snigula, J.M., "VIRUS: production of a massively replicated fiber integral field spectrograph for the upgraded Hobby-Eberly Telescope," Proc. SPIE, 8446-21 (2012)
[5] Tuttle, S.E., Hill, G. J., Vattiat, B. L., Lee, H, Drory, N., Kelz, A., Ramsey, J., Peterson, T., Noyola, E., DePoy, D. L., Marshall, J. L., Chonis, T. S., Dalton, G.B., Fabricius, M. H., Farrow, D., Good, J. M., Haynes, D. M., Indahl, B., Jahn, T., Kriel, H., Nicklas, H., Montesano, F., Prochaska, T., Allen, R. D., Landriau, M., MacQueen, P. J., Roth, M. M., Savage, R., Snigula, J. M. , "VIRUS early installation and commissioning.", Proc SPIE 9908-55 (2016)
[6] Hill, G.J., "HETDEX and VIRUS: Panoramic Integral Field Spectroscopy with 35k fibres" in 'Multi-Object Spectroscopy in the Next Decade' a conference held in La Palma, March 2015, (eds. I. Skillen, M. Balcells & S. Trager), ASP Conference Series, in press (2016)
[7] Hill, G.J., *et al*., "Current status of the Hobby-Eberly Telescope wide field upgrade," *Proc. SPIE*, 8444-19 (2012)
[8] Hill, G.J., Drory, N., Good, J., Lee, H., Vattiat, B.L., Kriel, H., Bryant, R., Elliot, L., Landiau, M., Leck, R., Perry, D., Ramsey, J., Savage, R., Damm, G., Fowler, J., Gebhardt, K., MacQueen, P.J., Martin, J., Ramsey, L.W., Shetrone, M., Schroeder, E., Cornell, M.E., Booth, J.A., and Moriera, W., "Deployment of the Hobby-Eberly Telescope Wide Field Upgrade", Proc. SPIE, 9145-5 (2014)
[9] Good, J.M., Hill, G.J., Leck, R.L., Landriau, M., Drory, N., Fowler, J.R., Kriel, H., Cornell, M.E., Booth, J.A., Lee, H., and Savage, R., "Laboratory Performance Testing, Installation, and Commissioning of the Wide Field Upgrade Tracker for the Hobby-Eberly Telescope", Proc. SPIE, 9145-156 (2014)
[10] John M. Good, Gary J. Hill, Martin Landriau, Hanshin Lee, Emily Schroeder-Mrozinski, Jerry Martin, Herman Kriel, Matthew Shetrone, James Fowler, Richard Savage, Ron Leck, "HET Wide Field Upgrade Tracker System Performance", Proc. SPIE 9906-167 (2016)
[11] Hill, G.J., Drory, N., Good, J.M., Lee, H., Vattiat, B.L., Kriel, H., Ramsey, J., Randy Bryant, R., Elliot, L., Fowler, J., Landiau, M., Leck, R., Odewahn, S., Perry, D., Savage, R., Schroeder Mrozinski, E., Shetrone, M., Damm, G., Gebhardt, K., MacQueen, P.J., Martin, J., Armandroff, T., Ramsey, L.W., "The Hobby-Eberly Telescope wide-field upgrade", Proc. SPIE 9906-5 (2016)
[12] Bacon, R., Accardo, M., Adjali, L., Anwand, H., Bauer, S., *et al.*, "The second-generation VLT instrument MUSE", Proc. SPIE 7735, 773508 (2010)
[13] Hill, G.J., Gebhardt, K., Komatsu, E., Drory, N., MacQueen, P.J., Adams, J.A., Blanc, G.A., Koehler, R., Rafal, Roth, M.M., Kelz, A., Grupp, F., Murphy, J., Palunas, P., Gronwall, C., Ciardullo, R., Bender, R., Hopp, U., and Schneider, D.P., "The Hobby-Eberly Telescope Dark Energy Experiment (HETDEX): Description and Early Pilot Survey Results", ASP Conf. Series, 399, 115 (2008)
[14] Burge, J.H., Benjamin, S.D., Dubin, M.B., Manuel, S.M., Novak, M.J., Oh, C.J., Valente, M.J., Zhao, C., Booth, J.A., Good, J.M., Hill, G.J., Lee, H., MacQueen, P.J., Rafal, M.D., Savage, R.D., Smith, M.P., and Vattiat, B.L., "Development of a wide-field spherical aberration corrector for the Hobby Eberly Telescope", Proc. SPIE, 7733-51 (2010)
[15] Oh, C.-J., Frater, E., Zhao, C., Burge, J.H., "System alignment and performance test of a wide field corrector for the Hobby-Eberly telescope", Proc. SPIE, 9145-8 (2014)
[16] Lee, H., Hill, G.J., Good, J.M., Vattiat, B.L., Shetrone, M., Martin, J., Schroeder Mrozinski, E., Kriel, H., Oh, C.-J., Frater, E., Smith, B., Burge, J.H., "Delivery, installation, on-sky verification of Hobby Eberly Telescope wide-field corrector," Proc. SPIE 9906-156 (2016)
[17] Good, J., *et al*., "Design of performance verification testing for HET wide-field upgrade tracker in the laboratory," Proc. SPIE, 7739-152 (2010)
[18] Vattiat, B.L., *et al*., "Design, testing, and performance of the Hobby Eberly Telescope prime focus instrument package," Proc. SPIE, 8446-269 (2012)
[19] Vattiat, B.L., Hill, G.J., Lee, H., Moreira, W., Drory, N., Ramsey, J., Elliot, L., Landriau, M., Perry, D.M., Savage, R., Kriel, H., Haeuser, M., and Mangold, F., "Design, alignment, and deployment of the Hobby Eberly Telescope prime focus instrument package", Proc. SPIE, 9147-172 (2014)
[20] H. Lee, *et al.*, "Analysis of active alignment control of the Hobby-Eberly Telescope wide field corrector using Shack-Hartmann wavefront sensors," Proc. SPIE, 7738-18 (2010)
[21] H. Lee, *et al*., "Metrology systems for the active alignment control of the Hobby-Eberly Telescope wide-field upgrade," Proc. SPIE, 7739-28 (2010)
[22] H. Lee, *et al*., "Metrology systems of Hobby-Eberly Telescope wide field upgrade," Proc. SPIE, 8444-181 (2012)

[23] Ramsey, J., Drory, N., Bryant, R., Elliott, L., Fowler, J., Hill, G. J., Landriau, M., Leck, R., Vattiat, B., "A control system framework for the Hobby-Eberly Telescope", Proc. SPIE, 9913-160 (2016)
[24] Hill, G.J., Nicklas, H., MacQueen, P.J., Tejada de V., C., Cobos D., F. J., and Mitsch, W., "The Hobby-Eberly Telescope Low Resolution Spectrograph", Proc. SPIE, 3355, 375 (1998)
[25] Chonis, T. S., Hill, G. J., Lee, H., Tuttle, S. E., and Vattiat, B. L., "LRS2: the new facility low resolution integral field spectrograph for the Hobby-Eberly Telescope," Proc. SPIE 9147-9 (2014)
[26] Chonis, T.S., Hill, G.J., Lee, H., Tuttle, S.E., Vattiat, B.L., Drory, N., Indahl, B.L., Peterson, T.W., Ramsey, J., "LRS2 – design, assembly, testing, and commissioning of the second generation low resolution spectrograph for the Hobby-Eberly Telescope", Proc. SPIE 9908-163 (2016)
[27] Vattiat, B., Lee, H., Chonis, T., Hill, G.J., Haubnitz-Reinke, C. "Design and Assembly of the Low Resolution Spectrograph 2 Integral Field Unit," Proc. SPIE 9908-138 (2016)
[28] Adams, J.J., Uson, J., Hill, G.J., and MacQueen, P.J., "A new z = 0 metagalactic UV background limit," ApJ, 728, 107 (2011)
[29] Adams, J.J., *et al*., "The HETDEX Pilot Survey I. Survey Design, Performance, and Catalog of Emission-Line Galaxies," ApJS, 192, 5 (2011)
[30] Blanc, G.A., et al., "The HETDEX Pilot Survey II: The Evolution of the Ly-α Escape Fraction from the UV Slope and Luminosity Function of 1.9<z<3.8 LAEs," ApJ, 736, 31 (2011)
[31] Tuttle, S.E., Hill, G.J., Lee, H., Vattiat, B.L., Noyola, E., Drory, N., Cornell, M.E., Peterson, T., Chonis, T.S., Allen, R.D., Dalton, G.B., DePoy, D.L., Edmonston, R.D., Fabricius, M.H., Kelz, A., Haynes, D.M., Landriau, M., Lesser, M.P., Leach, R.W., Marshall, J.L., Murphy, J.D., Perry, D., Prochaska, T., Ramsey, J., and Savage, R., "The construction, alignment, and installation of the VIRUS spectrograph", Proc. SPIE 9147-26 (2014)
[32] Marshall, J. L., DePoy, D. L., Prochaska, T., Allen, R. D., Williams, P., Rheault, J. P., Li, T., Nagasawa, D. Q., Akers, C., Baker, D., Boster, E., Campbell, C., Cook, E., Elder, A., Gary, A., Glover, J., James, M., Martin, E., Meador, W., Mondrik, N., Rodriguez-Patino, M., Villanueva, Jr., S., Hill, G. J., Tuttle, S., Vattiat, B., Lee, H., Chonis, T. S., Dalton, G. B., and Tacon, M., "VIRUS instrument collimator assembly," Proc. SPIE 9147-143 (2014)
[33] Kelz, A., Jahn, T., Haynes, D.M., Hill, G.J., Murphy, J.D., Rutowska, M., Streicher, O., Neumann, J., Nicklas, N., Sandin, C., Fabricius, M., and Tuttle, S.E., "HETDEX / VIRUS: testing and performance of 33,000 optical fibres", Proc. SPIE, 9147-269 (2014)
[34] Hill, G.J., Kelz, A., Murphy, J.D., Jahn, T., Haynes, D., Lee, H., Vattiat, B.L., M-Bauer, S., Drory, N., Tuttle, S.E., Neumann, J., Nicklas, H., Anwad, H., Fabricius, M.H., Montesano, F., Rutowska, M., Savage, R.D., Gebhardt, K., Roth, M.M., "The VIRUS 35k fiber system: design, fabrication, and characterization", Proceedings of *Fiber Optics in Astronomy IV*, PASP, submitted (2016)
[35] Kelz, A., Jahn, T., Hill, G. J., Tuttle, S. E., Vattiat, B. L., Bauer, S. M. et al., "Commissioning of VIRUS integral-field units at the Hobby-Eberly Telescope", Proc. SPIE, 9908-319 (2016)
[36] Indahl, B., Hill, G. J., Drory, N., Gebhardt, K., Tuttle, S. Ramsey, J., Ziemann, G., Chonis, T., Peterson, T., Peterson, A., Vattiat, B., Li, H., Hao, L., "VIRUS Characterization Development and Results from First Batches of Delivered Units", Proc. SPIE, 9908-299 (2016)
[37] H. Lee, et al., "VIRUS optical tolerance and production," Proc. SPIE, 7735-140 (2010)
[38] B. Vattiat, et al., "Mechanical design evolution of the VIRUS instrument for volume production and deployment," Proc. SPIE, 7735-264 (2010)
[39] Prochaska, T., *et al.*, "VIRUS spectrograph assembly and alignment procedures," Proc. SPIE, 8446-193 (2012)
[40] Tuttle, S.E., *et al*., "Initial results from VIRUS production spectrographs," Proc. SPIE, 8446-221 (2012)
[41] Chonis, T.S., Hill, G.J., Clemens, J.C., Dunlap, B., and Lee, H., "Methods for evaluating the performance of volume phase holographic gratings for the VIRUS spectrograph array," Proc. SPIE, 8446-209 (2012)
[42] Chonis, T. S., Frantz, A., Hill, G. J., Clemens, J. C., Lee, H., Adams, J. J., Marshall, J. L., DePoy, D. L., and Prochaska, T., "Mass production of volume phase holographic gratings for the VIRUS spectrograph array," Proc. SPIE 9151-53 (2014)
[43] Burgh, E.B., Bershady, M.A., Westfall, K.B., and Nordsieck, K.H., "Recombination Ghosts in Littrow Configuration: Implications for Spectrographs Using Volume Phase Holographic Gratings," PASP 119, 1069 (2007)
[44] Smith, M.P., Mulholland, G.T., Booth, J.A., Good, J.M., Hill, G.J., MacQueen, P.J., Rafal, M.D., Savage, R.D., and Vattiat, B.L., "The cryogenic system for the VIRUS array of spectrographs on the Hobby Eberly Telescope", Proc. SPIE, 7018-117 (2008)
[45] Chonis, T.S., *et al*., "Development of a cryogenic system for the VIRUS array of 150 spectrographs for the Hobby-Eberly Telescope," Proc. SPIE, 7735-265 (2010)

[46] Reiss, R., Deiries, S., Lizon, J.-L., and Rupprecht, G., "The MUSE instrument detector system", Proc. SPIE 8446, 84462P (2012)
[47] Murphy, J.D., Palunas, P., Grupp, F., McQueen, P.J., Hill, G.J., Kelz, A., and Roth, M.M., "Focal ratio degradation and transmission in VIRUS-P optical fibers", Proc. SPIE, 7018-104 (2008)
[48] Murphy, J.D., *et al*., "The Effects of Motion and Stress on Optical Fibers", Proc. SPIE, 8446-207 (2012)
[49] Snigula, J.M., *et al*., "Cure-WISE: HETDEX data reduction with Astro-WISE," Proc. SPIE, 8451-78 (2012)
[50] Snigula, J. M., Drory, N., Fabricius, M., Landriau, M., Montesano, F., Hill, G. J., Gebhardt, K., Cornell, M. E., "Cure-WISE: HETDEX Data Reduction with Astro-WISE", ASP Conf. Series, 485, 447 (2014)
[51] Lee, H., and Hill, G.J., "Image moment-based wavefront sensing for in-situ full-field image quality assessment," Proc. SPIE, 8450-191 (2012)
[52] Lee, H., Hill, G.J., Tuttle, S.E., and Vattiat, B.L., "Fine optical alignment correction of astronomical spectrographs via in-situ full-field moment-based wavefront sensing," Proc. SPIE, 8450-192 (2012)
[53] Lee, H., Hill, G.J., Tuttle, S.E., Noyola, E., Peterson, T., and Vattiat, B.L., "Field application of moment-based wavefront sensing to in-situ alignment and image quality assessment of astronomical spectrographs: Results and analysis of aligning 100 VIRUS unit spectrograph," Proc. SPIE, 9151-138 (2014).
[54] Prochaska, T., Allen, R., Rheault, J. P., Cook, E., Baker, D., DePoy, D. L., Marshall, J. L., Hill, G.J., and Perry, D., "VIRUS instrument enclosures," Proc. SPIE 9147-257 (2014)
[55] Grogin, N.A., et al., "CANDELS: The Cosmic Assembly Near-Infrared Deep Extragalactic Legacy Survey, ApJS, 197, 35 (2011)
[56] Bershady, M.A., Andersen, D.R., Harker, J., Ramsey, L.W., and Verheijen, M.A.W., "SparsePak: A Formatted Fiber Field Unit for the WIYN Telescope Bench Spectrograph. I. Design, Construction, and Calibration", PASP 116, 565 (2004)
[57] Bershady, M.A., "3D Spectroscopic Instrumentation" in '3D Spectroscopy in Astronomy, XVII Canary Island Winter School of Astrophysics', Cambridge University Press, Cambridge, (2009)
[58] Lawrence, J.S., Brown, D.M., Brzeski, J., Case, S., Colless, M., Farrell, T.J., Gers, L., Gilbert, J., Goodwin, M, Jacoby, G., Hopkins, A.M., Ireland, M.J., Kuehn, K., Lorente, N.P.F., Miziarski, S., Muller, R., Nichani, V., Rakman, A., Richards, S., Saunders, W., Staszak, N.F., Tims, J., Vuong, M., Waller, L.G., "The MANIFEST fibre positioning system for the Giant Magellan Telescope", Proc. SPIE 9147-341 (2014)